WIREs
NANOMEDICINE AND NANOBIOTECHNOLOGY WILEY

OVERVIEW

Probing the biological obstacles of nanomedicine with gold nanoparticles

Bin Li | Lucas A. Lane 🔾

Department of Biomedical Engineering, College of Engineering and Applied Sciences, Nanjing University, Nanjing, Jiangsu, China

Correspondence
Lucas A. Lane, Department of Biomedical Engineering, College of Engineering and Applied Sciences, Nanjing University, Nanjing, Jiangsu 210093, China.
Email: lucaslane@nju.edu.cn

Despite massive growth in nanomedicine research to date, the field still lacks fundamental understanding of how certain physical and chemical features of a nanoparticle affect its ability to overcome biological obstacles in vivo and reach its intended target. To gain fundamental understanding of how physical and chemical parameters affect the biological outcomes of administered nanoparticles, model systems that can systematically manipulate a single parameter with minimal influence on others are needed. Gold nanoparticles are particularly good model systems in this case as one can synthetically control the physical dimensions and surface chemistry of the particles independently and with great precision. Additionally, the chemical and physical properties of gold allow particles to be detected and quantified in tissues and cells with high sensitivity. Through systematic biological studies using gold nanoparticles, insights toward rationally designed nanomedicine for in vivo imaging and therapy can be obtained.

This article is categorized under:
    Nanotechnology Approaches to Biology > Nanoscale Systems in Biology

KEYWORDS
active targeting, cancer imaging, drug delivery, oncology, passive targeting

1 | INTRODUCTION

Nanomedicine has made a significant impact in the biomedical field due to nano-sized therapeutic and imaging agents demonstrating more favorable pharmacokinetics and biodistributions compared to small molecules (Kairdolf, Qian, & Nie, 2017; Peer et al., 2007; Smith & Gambhir, 2017; Sun et al., 2014a; Wilczewska, Niemirowicz, Markiewicz, & Car, 2012). However, nanoparticles generally still exhibit low delivery efficiencies with only 1% of an injected dose reaching target tissues (Wilhelm et al., 2016). As a result, many nanomedicines reaching the clinic have offered marginal benefits to patients (Arnedos et al., 2015; Friedman, Letai, Fisher, & Flaherty, 2015; Kim, Faix, & Schnitzer, 2017; Le Tourneau et al., 2015; Wilhelm et al., 2016). This delivery inefficiency arises from a series of biological obstacles that nanoparticles experience after intravenous administration (Blanco, Shen, & Ferrari, 2015; Chang et al., 2016; Hubbell & Chilkoti, 2012; Lane, Qian, Smith, & Nie, 2015; Nie, 2010). These biological obstacles include opsonization, clearance from the circulation by organs of the reticuloendothelial system (RES), tumor uptake and penetration, cellular internalization, and subsequent elimination from the body. The performance of nanoparticles when met with a biological obstacle is heavily influenced by the particle's physical dimensions and surface chemistry (Albanese, Tang, & Chan, 2012; Davis, Chen, & Shin, 2008; Jiang, Kim, Rutka, & Chan, 2008; Lane, Qian, Smith, & Nie, 2015; Petros & Desimone, 2010). Understanding the link between the physical and chemical properties of nanomedicine to their performance in overcoming in vivo obstacles can guide the rational design of

next-generation therapeutic and imaging agents offering significant improvement in benefits to patients. Gold nanoparticles are an excellent platform for pursuing studies to understand what properties are optimal to overcome physiological barriers. Gold nanoparticles are highly tuneable in their shape, size, and surface chemistry (Figure 1) (Yang, Yang, Pang, Vara, & Xia, 2015), and numerous well-established synthesis methods allow tuning of physical and chemical parameters independently and with great precision (Li, Zhao, & Astruc, 2014; Murphy et al., 2010; Obrien, Jones, Brown, & Mirkin, 2014; Wiley et al., 2005; Yang, Yang, et al., 2015). The shapes that can be achieved with gold nanoparticle syntheses cover a wide variety of unique and geometrical morphologies including spheres (Ruan, Shao, Shu, Wang, & Wu, 2014; Zheng et al., 2013; Zheng, Zhong, Li, & Xia, 2014), triangles (Chen et al., 2014a; Millstone, Hurst, Metraux, Cutler, & Mirkin, 2009; Scarabelli, Corona-dopuchau, Ginercasares, Langer, & Lizmarzan, 2014), cubes (Langille, Personick, Zhang, & Mirkin, 2012; O'Brien, Jones, Brown, & Mirkin, 2014), rods (And & Elsayed, 2003; And & Murphy, 2004; Ye, Zheng, Chen, Gao, & Murray, 2013), stars (Kumar, Pastorizasantos, Rodriguezgonzalez, De Abajo, & Lizmarzan, 2008; Niu, Chua, Zhang, Huang, & Lu, 2015), shells (Kalele, Gosavi, Urban, & Kulkarni, 2006; Pham & Jackson, 2002), disks (Millstone, Wei, Jones, Yoo, & Mirkin, 2008), and cages (Chen et al., 2005; Skrabalak et al., 2008). Monodisperse samples of these shapes can be prepared over a size range from a few nanometers to a few hundred nanometers. Gold particles can be easily functionalized with an assortment of bio-compatible coatings through strong and stable thiol binding (Love, Estroff, Kriebel, Nuzzo, & Whitesides, 2005; Trouiller, Hebié, el Bahhaj, Napporn, & Bertrand, 2015; Ulman, 1996). These biocompatible coatings can then be modified to display cellular affinity ligands on the surface such as small molecules (Dixit, Den Bossche, Sherman, Thompson, & Andres, 2006; Mansoori, Brandenburg, & Shakerizadeh, 2010), peptides (Chen et al., 2015; Gao et al., 2015; Ferro-Flores et al., 2015), anti-bodies (Chattopadhyay et al., 2012; Popovtzer et al., 2008), and aptamers (Dam et al., 2015; Huang, Sefah, Bamrungsap, Chang, & Tan, 2008; Kim, Jeong, & Jon, 2010; Melancon et al., 2014). Moreover, the physical and chemical properties of gold allows tracking of particles in biological systems using photoluminescence (Chen, Wang, Yuan, & Chang, 2015; Liu et al., 2016), surface-enhanced Raman scattering (Lane, Qian, & Nie, 2015; Qian, Ansari, & Nie, 2007), photoacoustic imaging (Li & Chen, 2015; Yang, Stein, Ashkenazi, & Wang, 2009), X-ray computed tomography (Dorsey et al., 2013; Shilo, Reuveni, Motiei, & Popovtzer, 2012), positron emission tomography (Frellsen et al., 2016; Sun et al., 2014b; Wang et al., 2012; Yang et al., 2017; Zhao et al., 2016), and Cerenkov luminescence imaging (Lee et al., 2016; Wang et al., 2013a). As gold is not an element occurring naturally in the body, it can be quantified with high sensitivity in cells and tissues using inductively coupled mass spectrometry or inductively coupled optical emission spectroscopy (Huang et al., 2008; Kim et al., 2010; Melancon et al., 2014). The bioinert characteristic of gold offers nanoparticle formulations that are essentially nontoxic and nonimmunogenic (Alkilany & Murphy, 2010; Shukla et al., 2005), thus gold nanoparticles are well suited for exploratory in vivo studies.

The focus of this review will be gold nanoparticle studies examining biological obstacles that are seen by intravenously administered nanomedicine including opsonization, cellular internalization, tumor accumulation, and elimination from the body. We place attention on intravenously administered particles as they have access to nearly all parts of the body that other systems cannot reach (Anselmo & Mitragotri, 2016), though other routes of administration (e.g., oral, inhalation, intradermal) experience similar biological obstacles to that of intravenously administrated particles. We will examine how physical and chemical properties of size, shape, and surface chemistry influence the behavior of nanoparticles when encountering these biological obstacles. Though the focus is on nanoparticles comprised of gold cores, in general particles that have similar size, shape, and surface chemistry will behave in a similar manner within biological environments regardless of the material that the core is made of (Otsuka, Nagasaki, & Kataoka, 2003). The understandings gained from studies using gold nanoparticles can lead to rationally designed nanomedicine based upon physical and surface chemical principles that hold no matter the core material composition.
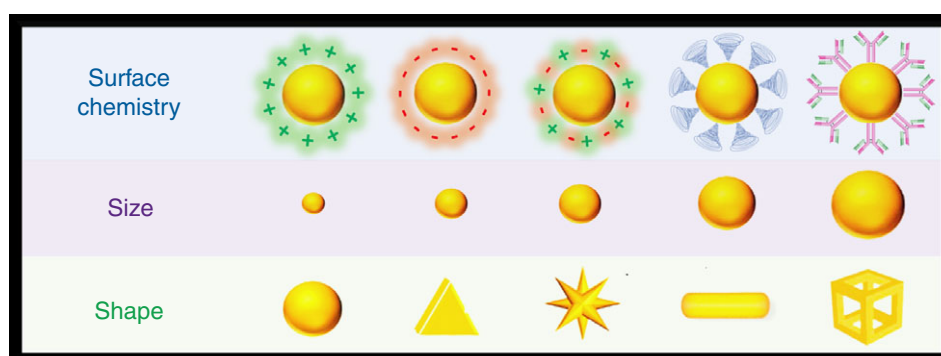

FIGURE 1 Gold nanoparticles can be tailored to a wide variety of sizes, shapes, and surface chemistries

2 | OPSONIZATION

When particles are introduced into the blood stream via intravenous administration, they experience millions of collisions with serum proteins each second (Lane, Qian, Smith, & Nie, 2015). These proteins can subsequently adsorb to the nanoparticle surface forming a protein shell, otherwise known as the "protein corona." (Cedervall et al., 2007; Lundqvist et al., 2008; Lynch & Dawson, 2008; Tenzer et al., 2013) The protein corona imparts a biological identity that can target nanoparticles for uptake by phagocytic cells within the RES organs (Caracciolo, Farokhzad, & Mahmoudi, 2017; Walkey, Olsen, Guo, Emili, & Chan, 2012). The process of protein corona formation in order to remove foreign agents from the blood is called opsonization (Cedervall et al., 2007; Karmali & Simberg, 2011; Lundqvist et al., 2008; Owens & Peppas, 2006; Vilanova et al., 2016). Opsonized particles trapped within RES organs are retained for long periods of time lasting several weeks to several months and hardly ever re-enter the blood stream (Cho et al., 2009; Thakor et al.,). For nanomedicine to be effective, opsonization must be avoided as it decreases the number of particles available to localize at diseased sites. Even worse, protein adsorption can also destabilize particles, causing them to aggregate (Ajdari, Vyas, Bogan, Lwaleed, & Cousins, 2017; Chakraborty et al., 2011; Deng, Liang, Monteiro, Toth, & Minchin, 2011; Dominguez-Medina et al., 2016). These aggregations can potentially clog blood vessels leading to restrictions in oxygen and nutrients to vital organs. The process of opsonization is influenced by physical dimensions and surface chemistry of particles (Lane, Qian, Smith, & Nie, 2015; Monopoli, Aberg, Salvati, & Dawson, 2012; Monopoli et al., 2011; Nel et al., 2009; Xia, Monteiroriviere, & Riviere, 2010). These properties affect the strength of forces attracting proteins to the surface of nanoparticles including Coulombic, van der Waals, and hydrophobic interactions (Lane, Qian, Smith, & Nie, 2015; Leckband & Israelachvili, 2001; Nath, Hyun, Ma, & Chilkoti, 2004; Walkey & Chan, 2012).

2.1 | Surface chemistry

The surface chemistry of a nanoparticle is dictated primarily by the type of coating used. Coatings can have a combination of charged and hydrophilic molecules that colloidally stabilize nanoparticles in media and prevent aggregation. These coatings also play an important role in how particles interact with biological species such as proteins and have a strong influence on whether opsonization occurs (Dobrovolskaia & McNeil, 2007; Elsabahy & Wooley, 2013; Moon, Huang, & Irvine, 2012). We note that coatings providing long-term colloidal stability in aqueous solutions do not always translate into coatings that are also colloidally stable in blood and resist opsonization. A classic example is citrate-coated gold nanoparticles which have long-term stability in aqueous solutions; however, when in the blood instantly become unstable and develop thick layers of adsorbed proteins (Dobrovolskaia et al., 2009). The propensity of a nanoparticle toward opsonization can be modified depending on the sign and magnitude of the surface charges and the hydrophilic character of the coating. Hydrophobic coatings are avoided in nanomedicine as they lead to poor particle stabilization and result in extensive protein adsorption and subsequent RES uptake (Lane, Qian, Smith, & Nie, 2015; Moyano et al., 2012).

A particle's surface charge, or zeta potential, has substantial impact on the degree of serum protein adsorption. Deng et al. (Deng, Liang, Toth, Monteiro, & Minchin, 2012a) examined how surface charge affects the extent of protein adsorption using polyacrylamide polymer coatings functionalized with either amine (positively charged), carboxyl (negatively charged), or hydroxyl (neutrally charged) surface groups. Both positively and negatively charged particles had a wider variety and greater amounts of adsorbed protein species than that of neutrally charged particles. Interestingly, the positively charged particles had lower affinity and faster release of serum proteins, most being negatively charged, than that of the negatively charged particles. Studies by Chandran et al. and Huhn et al. also observed serum protein binding favoring negatively charged particles over positively charged counterparts (Chandran, Riviere, & Monteiro-Riviere, 2017; Hühn et al., 2013). These results may seem counterintuitive when thinking about Coulomb's law stating like charges repel each other and opposites attract. However, experimental and molecular dynamics simulations have revealed that the attraction forces to negatively charged surfaces arising from small concentrated regions of positively charged lysine and arginine residues can outweigh repulsion forces of net global charges (Brewer, Glomm, Johnson, Knag, & Franzen, 2005). Charge neutral hydroxylated surfaces generally have less protein adsorption than charged surfaces, both positive and negative, as a result of better hydrogen bonding with water. With better surface hydration, proteins "see" a surface more like water and adsorption is less thermodynamically favored (Kairdolf, Mancini, Smith, & Nie, 2008; Lane, Qian, Smith, & Nie, 2015).

Zwitterions are another class of coatings that have a balance of positive and negative charges, resulting in a zero net charge. The resistance to protein adsorption in this case is believed to result by providing a hydrogen bonding network with water molecules and establishing a dense region of counterions to screen out any Coulombic attractions (Kane, 2003; Laughlin, 1991; Schlenoff & Zwitteration, 2014; Shao & Jiang, 2013; Shao & Jiang, 2014; Shao, White, & Jiang, 2014). Nowinski et al. developed zwitterionic coatings consisting of peptides with alternating anionic glutamic acid and cationic lysine amino acid residues (Nowinski, White, Keefe, & Jiang, 2014). The alternating sequences of glutamic acid and lysine form a strong

hydration layer for proteins and are the two most prevalent amino acid residues presented on their surfaces (Chen, Cao, & Jiang, 2009; White et al., 2012). The particles were tested for stability in undiluted human serum for 24 hrs at physiological temperatures. The particles maintained their original hydrodynamic diameters (HDs), indicating that little to no protein adsorption has occurred and that the particles did not aggregate. Another biological zwitterion, glutathione, has also been observed to prevent nonspecific binding of proteins (Vinluan et al., 2014). However, the resistance to protein adsorption of glutathione coatings has only been seen for small (1–3 nm) gold clusters. Zwitterions consisting of sulfobetaines and carboxybetaines have been previously shown to have superior resistance to protein adsorption on solid surfaces (Jiang & Cao, 2010; Kane, 2003). Using polymers with cross-linkable side chains displaying carboxybetaine on the surface was used to stabilize gold nanoparticles by Jiang et al. (Yang et al., 2014a) Here particles maintained their hydrodynamic sizes in human serum indicating great stability and resistance to protein adsorption. We note that not all zwitterions are equal in their ability to maintain the stability of particles within biological environments. Cysteine, a zwitterionic amino acid displaying amine and carboxyl groups, is observed to offer poor stability to gold nanoparticles, leading to aggregation when placed in biological media (Acres, Feyer, Tsud, Carlino, & Prince, 2014; Aryal, Remant Bahadur, Bhattarai, Kim, & Kim, 2006). Interestingly, Ning et al. found that if a glycine residue is added to cysteine, gold particles become physiologically stable and exhibit little to no protein adsorption (Ning et al., 2017). In this case adding the glycine residue creates a larger molecular separation between the amine and carboxyl groups with little addition to the overall HD (~0.4 nm). The differences in the performance among zwitterions can be differences in the molecular spacing between oppositely charged groups and how robust the formal charges are under changing environmental conditions. Both of these properties are expected to affect the structure of the surface hydration layer.

Polyethylene glycol (PEG) has been a staple coating for preventing nonspecific protein adsorption (Petros & Desimone, 2010; Yoo, Chambers, & Mitragotri, 2010). These polymers resist protein adsorption by displaying hydrated surfaces in addition to acting like "entropic springs" that repel proteins away from material surfaces (Lane, Qian, Smith, & Nie, 2015; Leckband, 2000). In a study by Johnston et al. they compared a variety of coatings on 5-nm gold particles (Johnston et al., 2017). The coatings examined were citrate, bis(p-sulfanatophenyl)phenylphosphine (BSPP), PEG, dodecylamine-grafted poly(isobutylene-alt-maleic anhydride) (DDA-PIMA), and dodecylamine grafted poly(isobutylene-alt-maleic anhydride) grafted with PEG (DDA-PIMA-PEG). Here they found that the ionically stabilized particles of citrate and BSPP showed poor colloidal stability and had an abundance of proteins adsorbed to the surface of the particles. Though the polymeric DDA-PIMA ligands performed better than the ionically stabilized particles, perhaps due to an entropic spring effect, the particles with PEG displayed on the outer surface (DDA-PIMA-PEG) were observed to have the least amount of adsorbed proteins. In an expansive study by Chan et al. (Walkey et al., 2014), 105 different coatings on gold nanoparticles were analyzed for nonspecific protein adsorption. In general, PEG coatings with a neutral surface charge outperformed those having an overall anionic or cationic charge. This trend held whether the charged coatings were large polymers, small molecule, or even PEG molecules with charged surface moieties. A simple change in the moiety on the surface of PEG molecules from a hydroxyl to a carboxyl group can lead to significant changes in the molecule's ability to resist protein adsorption. Davidson et al. found hydroxyl-terminated PEG coatings resisted adsorption of blood albumins completely whereas carboxyl-terminated PEG coatings had similar amounts of protein adsorbed to the surface as citrate-coated particles (Davidson, Brust, Cooper, & Volk, 2017). Though the proteins on the surface of carboxyl-terminated PEG coatings adhered with significantly less affinity than citrate-coated particles. Since the prevention of nonspecific binding by PEG is partly attributed to an entropic spring mechanism, one would presume that a certain molecular weight (or length) of PEG polymers would be required. Indeed, studies by Walkey et al. and Cui et al. found that PEG polymers of at least 5 kDa are needed to prevent protein coronas from forming (Cui et al., 2014; Walkey et al., 2012). In the study by Cui et al. they found that smaller PEG molecular weights of 2 kDa, though having some protein adsorption, still outperformed coatings of citrate, thioglycolic acid, and cysteine (Cui et al., 2014). Only in cases where particle sizes are a few nanometers, coatings of PEG molecules with molecular weights around 200 Da have been observed to resist protein adsorption (Zheng, Davidson, & Huang, 2003; Zheng, Li, & Huang, 2004). This may be a result of smaller particles having less affinity toward proteins.

After establishing a coating to resist nonspecific binding of proteins, many nanomedicine constructs also incorporate cellular affinity ligands to the surface in aims for specific cellular targeting (Debbage, 2009; Moderypawlowski & Gupta, 2014; Richards, Maruani, & Chudasama, 2017). However, these molecules do not have the same surface chemistry as the underlying coating and can potentially increase the susceptibility of the nanoparticle to opsonization. If the opsonization is excessive, the protein layer can interfere or even completely prevent the affinity ligand from binding to its target. In a study by Xiao et al., they found that adding affinity ligands would increase the protein adsorption on gold nanoparticles compared to those with solely PEG coatings (Xiao et al., 2018). Affinity ligands that the authors compared were RGD peptides and transferrin proteins, both of which can target nanoparticles to a variety of cancer cells. The smaller RGD ligands' affinity was affected more by protein adsorption than that of the larger transferrin proteins. This result is likely due to the protein layer being thick

enough to cover and block RGD activity but not enough to prevent the larger transferrin molecules. Huang et al. compared PEGylated gold nanorods with targeting ligands of RGD and antibody fragments (Huang et al., 2010). Here they found that the smaller molecules of RGD affected the nonspecific binding properties of PEG less than the larger targeting molecules of antibody fragments. Too many targeting ligands on the surface will allow nonspecific binding to an extent that may eliminate the specific cellular affinity of the nanoparticle and eliminate the prevention of nonspecific binding offered by the underlying coating. Small molecules, though their affinity is affected more by a protein corona, have less of a footprint on the surface and have less interference with a coating's ability to prevent protein adsorption. Thus, one needs to optimize particles for affinity ligand density to enhance specific targeting, but also to prevent nonspecific binding in order to maintain the specific targeting ability.

2.2 | Size

Size can affect several aspects of the protein corona including its thickness and the composition of the various proteins comprising the layer (Deng, Liang, Toth, Monteiro, & Minchin, 2012b; Gunawan, Lim, Marquis, & Amal, 2014; Lacerda et al., 2010; Mahmoudi et al., 2011). In a study by Deng et al., the affinity of the protein fibrinogen to negatively charged poly-acrylic acid-coated gold nanoparticles was examined (Deng et al., 2012b). The authors observed that particles within the size range of 7–22 nm, the binding affinity increased and had a slower dissociation rate with increasing diameter. The increased adsorption of proteins with size is not an unexpected phenomenon. The van der Walls attraction potential between proteins and similarly sized nanoparticles scales with their radii (Lane, Qian, Smith, & Nie, 2015). In addition to greater attraction potentials, larger particles have greater surface area for the protein to interact with and adsorb onto. Kaur and Forrest found that larger particles will also exhibit greater surface densities of adsorbed proteins (Kaur & Forrest, 2012). This result indicates that the increased amount of proteins adsorbed to larger particles is not solely due to having more available surface area. In addition to increased affinity of proteins toward larger particles, Lacerda et al. have also observed increased binding cooperativity (Lacerda et al., 2010). Though as particles became larger than 50 nm, the increases of protein adsorption with increasing diameter began to diminish. This can be a result of the decreasing curvature of the particles. Beyond 50 nm particles sizes, the conformations available to the adsorbed protein may not differ from that of a flat surface. Additionally, as the size difference between the particle and protein become significantly different, the van der Waals attraction potential gains with increasing size become negligable (Lane, Qian, Smith, & Nie, 2015). Most blood proteins have a HD between 3 and 15 nm (Rahman, Laurent, Tawil, Yahia, & Mahmoudi, 2013).

2.3 | Shape

Though much less studied, the shape of a nanoparticle can have an impact on the adsorption of proteins (Gagner, Lopez, Dordick, & Siegel, 2011; Ma, Bai, Wang, & Jiang, 2014; Zhou et al., 2009). A study by Garner et al. compared the protein adsorption between gold spheres of 11 nm and gold nanorods of 10 × 36 nm (Gagner et al., 2011). The authors found that nanorods exhibited 10 times greater protein adsorption than the spheres. The greater adsorption of proteins to the nanorods may be a combination of the nanorods having three times the surface area and a lower surface curvature compared to the spheres. Goy-Lopez et al. found that albumins had greater changes in their secondary and tertiary structure upon adsorbing to particles with lower curvatures (Goy-López et al., 2012). This denaturation process upon adsorption can reveal different surface chemical characteristics and epitopes that can alter the extent and composition of subsequent proteins adsorbing to the surface. Moreover, denatured proteins may adopt configurations having higher binding affinity. Examining this effect on particles with the same size and surface chemistry but different surface curvatures, such as comparing spheres and disks, on the protein adsorption level, binding affinity, and extent of denaturation would be an interesting exploration (Figure 2).

3 | CELLULAR INTERNALIZATION

For external substances to enter cells, they must cross the cell membrane. However, cell membranes are impermeable to diffusion by most nano-sized agents. Therefore, nanoparticles rely on endocytosis for cellular entry (Conner & Schmid, 2003; Hillaireau & Couvreur, 2009; Yameen et al., 2014). The desire for or against endocytosis depends on the nanomedicine's application. Specific cellular endocytosis is important for therapeutic applications where either free drug molecules exhibit widespread systemic toxicity (resulting from low cellular specificity) or are unable to enter cells due to being insoluble (Akinc & Battaglia, 2013; Ruoslahti, Bhatia, & Sailor, 2010). Avoiding nonspecific cellular internalization is also important to avoid systemic toxicity. In imaging applications, avoidance of cellular internalization is generally desired in order to allow efficient elimination from the body (Yu & Zheng, 2015).
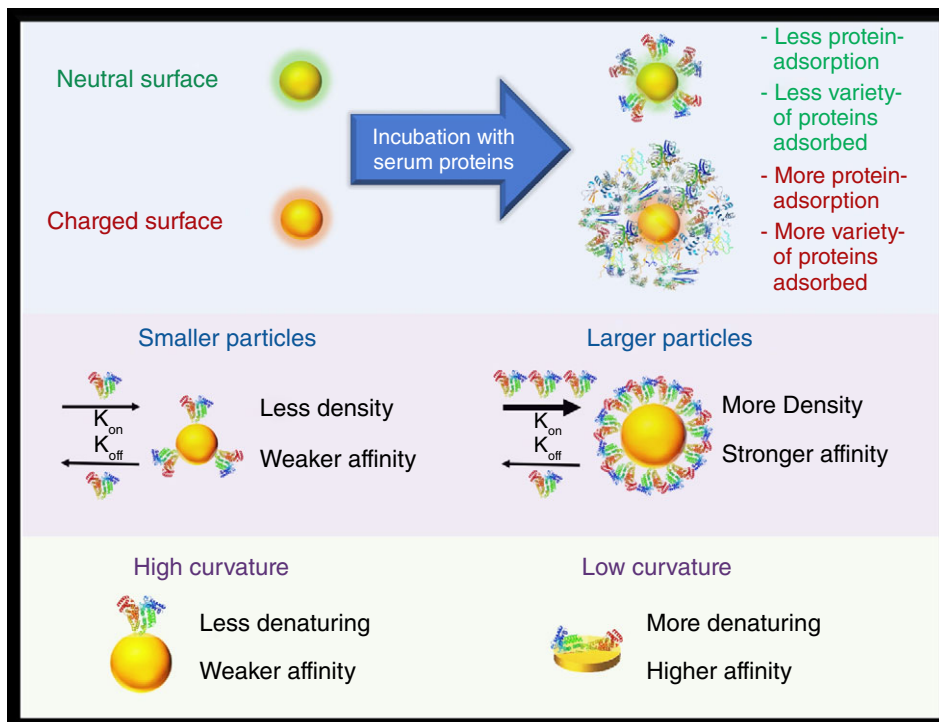
FIGURE 2 Nanoparticles with neutral coatings (zeta potential near zero) tend to have less protein adsorption and fewer adsorbed species compared to counterparts having charged (anionic or cationic) surfaces. Proteins adsorb with less affinity and less surface density to smaller particles than larger particles. Proteins have less affinity and are less prone to denature on particle morphologies having higher curvatures

3.1 | Surface chemistry

Surface chemistry plays a large role in the ability of a cell to internalize nanoparticles. The combination of Coulombic, Van der Waals, and hydrophobic forces are at play when nanoparticles interact with cells just as they are when interacting with proteins (Lane, Qian, Smith, & Nie, 2015). Thus, similar principles in modifying the extent of protein adsorption can be applied to modify the extent of cellular internalization. For instance, nonspecific interactions between nanoparticles and cells are also minimized through the use of zwitterionic coatings or hydrophilic polymers (Lane, Qian, Smith, & Nie, 2015). However, new phenomena arise in nanoparticle-cell studies as the particles encounter a viable entity and its processes of endocytosis.

In contrast to the counterintuitive results seen with Coulombic interactions between nanoparticles and proteins, cellular studies generally follow more closely to what would be expected. In many cases, positively charged gold particles are observed to have higher cellular uptake than negatively or neutrally charged couterparts (Cho, Xie, Wurm, & Xia, 2009; del Pino et al., 2016; Hauck, Ghazani, & Chan, 2008; Hühn et al., 2013; Liang et al., 2010; Mosquera et al., 2018; Oh & Park, 2014a; Ojeajimenez, Garciafernandez, Lorenzo, & Puntes, 2012). The increased internalization of positively charged particles is commonly attributed to the favorable electrostatic interactions to the negatively charged cellular membrane. However, endocytosis of nanoparticles has been seen to increase with the number of positively charged groups on nanoparticle surfaces rather than the magnitude of the zeta potential. del Pino et al. found that gold particles with more quaternary ammonium groups on the surface had a greater propensity to be internalized by cells, even for samples having similar zeta potentials (del Pino et al., 2016). Though these results still follow Coulomb's law, they suggest local interactions between charged groups on the surface of a nanoparticle, and the molecules on the cell membrane have more influence than global attractions via opposite zeta potentials. Increasing the uptake of nanoparticles based on charge limits targeting to specific cellular types, thus this strategy will generally not be suitable for therapeutic or imaging applications. Once particles are internalized, their surface chemistry can also dictate whether the particle remains within the cell or has the ability to be exocytosed. Studies conducted by Oh and Park compared gold nanoparticles with cationic, anionic, zwitterionic, and PEG coatings for their ability to exit cells after internalization (Oh & Park, 2014a; Oh & Park, 2014b). Their results indicated that internalized PEG coated particles had the greatest chances of being exocytosed with near 80% able to exit cells within a 48 hr period. Particles with anionic and zwitterionic coatings followed PEG with over 50% of the internalized sample leaving the cells within the same time period. Cationic particles were the least likely to leave cells once internalized having only 20% of the sample exocytosed. The exocytosis of nanoparticles was observed to be linked to the colloidal stability within endosomes. Cationic particles were seen to aggregate into large structures which limited the cell's ability to remove the particles. PEG-coated particles were seen to have the least interactions with proteins of the endosome, thus were more likely to preserve a smaller size more suitable for leaving the cell.

Coatings that are better at resisting nonspecific binding not only limit the number of particles that are internalized by cells, but also prevent prolonged retention of the particles if they do get internalized by a nontarget cell.

Once introduced within the body, nanoparticle surfaces have some level of protein adsorption. To model intravenously administered particle interactions with cells in vivo, samples can be incubated with serum proteins within cellular cultures. The adsorption of proteins on the surface of particles is seen to alter the extent of uptake. Generally, increased levels serum protein adsorption lead to increased levels of internalization (Arnida, Janát-Amsbury, Ray, Peterson, & Ghandehari, 2011; Melby et al., 2017). This trend has been shown in an extensive study performed by Walkey et al. where 105 different surface coatings were inspected for protein adsorption and subsequent cellular internalization (Walkey et al., 2014). Here, particles having coatings better at preventing nonspecific binding of proteins were also better at preventing subsequent nonspecific cellular uptake. Though nonspecific protein adsorption is normally associated with increased cellular uptake, there have been cases where particles are internalized to a lesser extent upon protein adsorption. Monteiro-Riviere et al. have observed a decrease in uptake of gold nanoparticles after particles developed protein coronas (Chandran et al., 2017; Choi, Riviere, & Monteiro-Riviere, 2017; Li & Monteiro-Riviere, 2016). This effect has been observed by their group with different cell types (keratinocytes, hepatocytes, and human umbilical vein endothelial cells) and particles with anionic, cationic, and even PEG coatings. Cheng et al. also observed decreases in macrophage uptake by PEGylated gold particles that were preincubated with serum proteins (Cheng et al., 2015). Furthermore, some have even suggested that protein adsorption is necessary for PEG-coated particles to resist nonspecific cellular binding; however, it seems that particular protein corona compositions are needed see this effect (Schöttler et al., 2016). We caution that these results can be conflicting due to different nanoparticle preparations. For instance, different samples may have different grafting densities of polymers on the surface. Walkey et al. found high grafting densities are required for PEG to resist protein adsorption onto gold nanoparticles, and the reductions in protein adsorption are seen to correlate with decreased uptake into macrophage cell lines (Walkey et al., 2012). This observation has been made with particle cores composed of materials other than gold as well (Lee & Larson, 2016; Yang et al., 2014b). Particles with sparse PEG coatings on the other hand may benefit from protein adsorption, since proteins tend to provide better colloidal stability than a bare nanoparticle surface (Lee & Larson, 2016; Yang et al., 2014b). There are certain proteins found within membranes of blood cells that can actively prevent the uptake of nanoparticles. In particular, CD47 which is found on red blood cell surfaces acts as a "don't eat me" signal to macrophages (Oldenborg et al., 2000; Tsai, Rodriguez, & Discher, 2010). Gao et al. found that red blood cell membranes having CD47 markers can be utilized as surface coatings for gold nanoparticles to reduce macrophage uptake (Gao et al., 2013). Using 70-nm gold particles, the red blood cell membrane coatings reduced macrophage uptake over fourfold compared to citrate coated counterparts. Whether further reduction in cellular uptake can be achieved using coatings having a combination of molecules that resist nonspecific binding with biologically active proteins signaling "don't eat me" has yet to be explored.

Specific cellular internalization can be promoted by using affinity ligands. Here molecules which recognize specific cellular surface receptors are tethered to the surface of nanoparticles. Once the ligands meet their complementary receptors, it can trigger a variety of active transport mechanisms leading to internalization (Behzadi et al., 2017). Several groups have demonstrated the ability of affinity ligands to increase uptake within cells expressing the specific molecular targets for the ligand (Antosh et al., 2015; Au et al., 2008; Au et al., 2010; Guo, O'Driscoll, Holmes, & Rahme, 2016; Hu et al., 2009; Huang et al., 2010; Melancon et al., 2008; Pissuwan, Valenzuela, Killingsworth, Xu, & Cortie, 2007; Rejiya, Kumar, Raji, Vibin, & Abraham, 2012; Yang, Uertz, Yohan, & Chithrani, 2014). Moreover, specific interactions lead to greater internalization of nanoparticles than nonspecific interactions. For instance, antibody-coated particles have been observed to be internalized within their cellular targets four to eight times more efficiently than positively or negatively charged particles (Charan et al., 2012). We note that nonspecific interactions are still present and influence the affinity between cells and targeted nanoparticles. In a study by Yin et al., they observed that negatively charged particles with antibodies on the surface had less affinity to their cellular targets than free antibodies (Yin et al., 2015). This effect was attributed to the Coulombic repulsion between the negatively charged surfaces of the particle and the cell. PEG and other coatings preventing nonspecific binding, though inhibiting opsonization and subsequent macrophage uptake, may also decrease the interactions necessary for target cells to internalize particles (Harrison et al., 2016; Li & Huang, 2008). This typically occurs when polymers extend beyond that of the affinity ligand (Lane, Qian, Smith, & Nie, 2015). A method to resolve this issue was performed by Chan and colleagues who used smaller PEG ligands to surround PEG ligands attached to antibodies at their distal ends, thereby maintaining the specific binding of the affinity ligand while maintaining the nonspecific binding protection of a dense PEG coating (Dai, Walkey, & Chan, 2014).

3.2 | Size

Nanoparticle size affecting cellular internalization was demonstrated in a pioneering study by Chithrani et al. (Chithrani, Ghazani, & Chan, 2006) In this study, citrate-coated gold nanoparticles having sizes 14, 30, 50, 74, and 100 nm were

incubated with HeLa cells for 6 hrs. They found that particles of 50 nm in size had the greatest uptake among the sizes inspected. As particles became smaller or larger, the uptake efficiency steadily decreased from around 6,000 nanoparticles (NPs) per cell to 2,000 NPs per cell. Theoretical analyses supported these observations showing particle sizes near 50 nm would have higher uptake efficiencies than their larger and smaller counterparts as larger particles require cell membranes to wrap around a larger surface area taking more time and smaller particles require adopting membrane invaginations of higher curvature costing more energy (Decuzzi & Ferrari, 2007; Gao, Shi, & Freund, 2005; Zhang, Li, Lykotrafitis, Bao, & Suresh, 2009). However, changes in the surface chemistry of particles have been found to change the optimal size for cellular uptake. Liu et al. observed that optimal sizes for uptake depend on the surface charge (Liu, Huang, Li, Jin, & Ji, 2013). Using particle sizes ranging from 16 to 58 nm, uptake continued to increase as size increased for positively charged particles, whereas 40 nm particles had greater uptake for negatively charged particles.

There also have been a number of studies that indicate smaller particle sizes are internalized by cells to a greater extent than larger ones when the particles are in the 10–100 nm size range. Wong and Wright examined the size effects on uptake using negatively charged DNA functionalized gold nanoparticles (Wong & Wright, 2016). Using particles having HDs ranging from 20 to 60 nm, they found 60 nm particles had a near threefold reduction in uptake compared to smaller 20 nm counterparts. When using similar gold core sizes of 15 nm and changing the HD by modifying the thickness of the DNA coating, the 60 nm-sized particles also saw a reduction (twofold) in uptake compared to 20 nm particles. Conflicting with the observations by Liu et al. for positively charged particles (Liu, Huang, et al., 2013), Elbakry et al. reported near 10-fold decreases in cellular internalization as HDs increased from 32 to 85 nm (Elbakry et al., 2012). Cho et al. observed higher cellular uptake for smaller 15 nm gold particles compared to larger 45 nm particles regardless of surface chemistry, whether PEG or amine coated or antibody targeted (Cho, Au, Zhang, & Xia, 2010). Interestingly, Jiang et al. found that once particles reach sizes as small as 2 nm, zwitterionic coatings that prevent uptake for larger-sized particles are observed to be uptaken at similar rates as cationic and anionic coatings (Jiang et al., 2015). Though at the 1–10 nm size range, larger cationic and anionic particles tend to be internalized at higher rates.

The differences in optimal sizes for internalization within cells are strongly tied to the nanoparticle's surface chemistry. Particle surfaces with strong affinity for the cellular membrane can change the thermodynamic landscape for internalization, allowing wrapping of smaller particles to become more energetically favorable and larger particles to be wrapped in shorter times. A more consistent finding among reports is particles in size ranges of 10–100 nm will have greater internalization than particles outside this range. Particles that are too small may cost too much cellular energy to be internalized by endocytosis. This would leave diffusion through the membrane as the only transport method for such small particles. Diffusion is significantly slower than endocytosis, thus using small particle sizes offers a possible method to evade nonspecific uptake by cells of the RES. However, if therapy is the goal, the particles may also experience difficulty entering their intended cellular targets. On the other hand, particles that are larger than 100 nm may be at sizes beyond which vesicles formed by most endocytic mechanisms can accommodate (Behzadi et al., 2017; Oh & Park, 2014b). This would leave these large particles to engulfment by specialized phagocytic cells that can handle large foreign materials such as macrophages. In most applications in nanomedicine, particle engulfment by phagocytes is undesirable as this leads to greater accumulation and retention of particles in off-target organs, leading to concerns of both acute and chronic toxicity.

3.3 | Shape

Shape may have less of an influence compared to other parameters when it came to protein adsorption; however, it has a significant influence on cellular internalization. Studies on differences in particle uptake based on shape were pioneered by Chithrani et al. who examined quasi-spherical and rod-shaped particles (Chithrani et al., 2006; Chithrani & Chan, 2007). An interesting finding was that gold nanorods with dimensions of 14 × 74 nm had reduced uptake than quasi-spherical particles of 14 and 74 nm sizes where the reduction was threefold and fourfold, respectively. Another finding of their studies was that uptake tended to decrease as the aspect ratio of the particles increased. We note that the spherical particles and rods had different surface chemistries in these studies where the rods were positively charged while the spherical particles were negatively charged. However, in most cases positively charged particles tend to be internalized by cells more efficiently than negatively charged particles, thus shape may have a greater control of uptake efficiency than the surface charge of the particle. Subsequent studies have also reported decreased uptake of nanorods compared to spherical counterparts even when the surface chemistry is the same (Arnida et al., 2011; Bartczak et al., 2012; Tarantola et al., 2011). For example, Arnida et al. observed 50-nm PEGylated spheres to have four times the uptake than PEGylated gold nanorods having dimensions of 10 × 45 (Arnida et al., 2011). Additionally Bartczak et al. reported PEGylated 15 nm spherical particles having greater uptake into cells than PEGylated nanorods of dimensions of 17 × 47 nm (Bartczak et al., 2012). From these reports, it seems nanorods have less internalization than spherical counterparts that have comparable dimensions to either the length or the diameter of the nanorod. Currently, the accepted theory as to why particles with greater aspect ratios are internalized less by cells is that the cell can only partially wrap its membrane around such particles (Decuzzi & Ferrari, 2008). Particles with increased aspect ratios
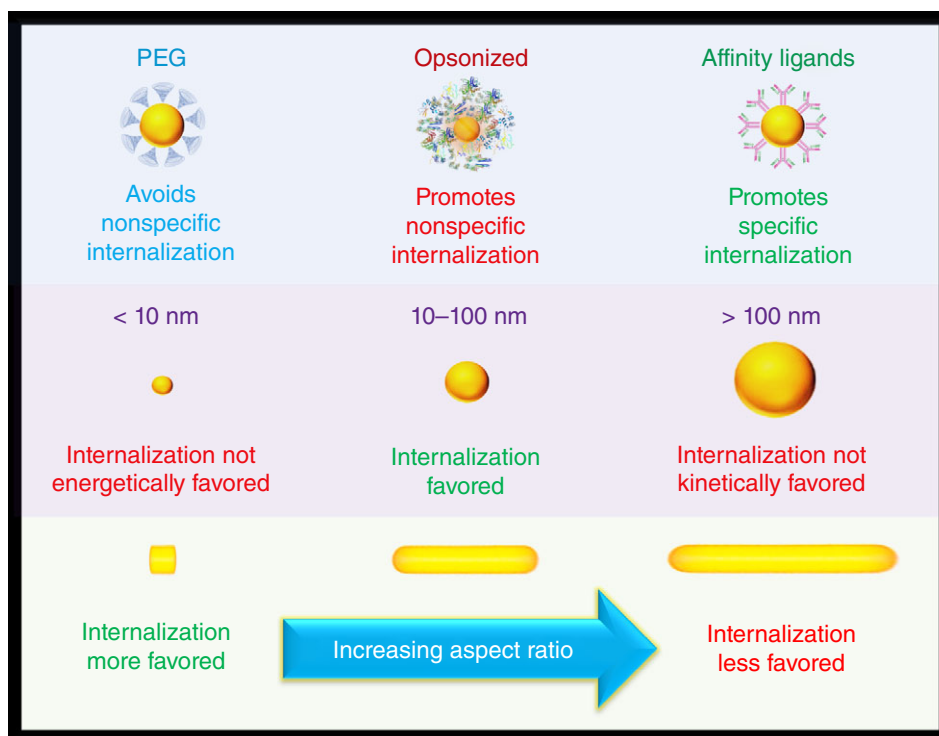
FIGURE 3 Particle coatings that prevent nonspecific binding of proteins such as PEG, also provide particles with protection against nonspecific cellular internalization. Opsonized particles on the other hand are highly likely to be nonspecifically internalized by cells. Affinity ligands on the surface of particles aid in the internalization of particles within specific cells having surface receptors complimentary to the ligand. Particles that are smaller than 10 nm do not have efficient cellular internalization due to the membrane having to adopt a shape with high curvature which is not energetically favored. Particles within the 10–100 nm size range are at sizes that the cellular membrane can accommodate and wrap around in a short period. Internalization is not kinetically favored for particles that are larger than 100 nm due to the long wrapping times required to cover the significantly larger surface areas. When increasing the aspect ratio of a particle, internalization becomes less efficient as the membrane must adopt configurations with greater surface area to volume ratios which are not energetically favored

require membranes to adopt configurations with greater surface area to volume ratios which are not energetically favored. As the membrane cannot fully wrap around the particle, it cannot be internalized efficiently. This process has been dubbed "frustrated endocytosis." Hence, shape can be employed as a means to prevent nonspecific cellular internalization in addition to applying "stealth" coatings such as PEG.

There have been conflicting results reporting nanorods having a greater propensity for cellular uptake over spherically shaped counterparts. Cho et al. compared citrate and PEG coated 17 nm particles to that of CTAB- and PEG-coated nanorods of 50 × 20 nm (Cho, Liu, & Xia, 2010). The citrate-coated spheres and CTAB-coated nanorods had similar uptake levels; however, differences were observed when the particles were PEGylated. PEGylated spheres had a fourfold reduction compared to their citrate-coated counterparts while the nanorods had a twofold reduction in uptake compared to their CTAB-coated counterparts. In this case, PEGylated nanorods had twice the uptake levels than PEGylated spheres. We note that conflicting results may be a result of the efficiency of PEGylation of the nanoparticle samples. In most studies, spherical particles as-synthesized commonly have citrate coatings whereas nanorods are as-synthesized coated with CTAB. CTAB is harder to replace on gold surfaces than citrate (Xia et al., 2012), therefore nanorods may not have the same PEG grafting density as the spherical particles in a study. In cases of insufficient PEGylation of nanorods, the increased number of leftover CTAB on the nanorod surface may be the reason for increased uptake rather than a shape-based effect. Additionally, we caution that the coatings applied to anisotropic nanoparticles can change the aspect ratio. Typically, thick coatings of PEG are used to prevent nonspecific uptake of particles. Increasing PEG thickness will lead to lowering the aspect ratio of the particle in terms of its hydrodynamic dimensions, leading to a more spherical particle "seen" by the cell. Therefore, we expect that as thicker coatings are applied to particles, the differences in uptake levels between anisotropic and spherical particles will be diminished (Figure 3).

4 | TUMOR ACCUMULATION

Much of the research efforts in nanomedicine has been dedicated toward the delivery of therapeutic and imaging agents to cancerous tumors. These dedicated efforts are in part due to preferential accumulation of intravenously administered

nanoparticles within tumor tissues over normal tissues. This preferential accumulation is a result of the pathophysiology of tumor tissues. Tumor blood vessels are highly irregular and usually have large fenestrations (Danquah, Zhang, & Mahato, 2011; McDonald, Thurston, & Baluk, 1999; Mei, Bai, Lorrio, Wang, & Al-Jamal, 2016). Such vessels have greater permeability for nanosized materials than normal vessels (Weis & Cheresh, 2011). Additionally, tumors tend to have impaired lymphatic drainage which leads to retention of the permeated nanoparticles (Miao & Huang, 2015). The combination of these conditions leading to the increased uptake of nanoparticles within tumors is called the enhanced permeation and retention (EPR) effect (Iyer, Khaled, Fang, & Maeda, 2006). Yet, the accumulation within tumor tissues can be either further enhanced or diminished depending on the physical dimensions and surface chemistry of the nanoparticle.

4.1 | Surface chemistry

Particles that have surface chemistries that are prone to nonspecific protein adsorption and subsequent nonspecific cellular uptake are removed from the circulation at quicker rates, thus diminishing the number of particles available in the blood to reach tumor sites. Therefore, a common method in evaluating the in vivo performance of nanoparticles is not only to evaluate the accumulation at the tumor site, but also to examine the blood concentration of the particles with time. Evaluating the concentration of the particles in the circulation over time is an indirect evaluation of the ability of the particles to avoid opsonization and clearance by the RES organs. Charged particles tend to exhibit greater nonspecific binding compared to those of neutral or zwitterionic coatings leading to accelerated clearance of the particles from the blood stream. A study by Arvizo et al. evaluated the circulation kinetics of gold particles with either neutral, cationic, anionic, or zwitterionic coatings (Arvizo et al., 2011). All the coatings had the same anchors of thiolated tetraethylene glycol where the only differences were the charge groups on the surface consisting of either hydroxyl, quaternary ammonium, carboxyl, or sulfobetaine groups. Additionally, all of the particles had similar HDs (~10 nm). The plasma concentrations for the zwitterionic and neutral particles were considerably greater over time than their cationic or anionic charged counterparts with their areas under the curve being an order of magnitude larger. This increase in blood concentration overtime leads to fivefold increases in particle concentrations within tumors. One of the most widely used polymers to prolong the circulation of particles is PEG (Lane, Qian, Smith, & Nie, 2015; Lin, Monteiroriviere, & Riviere, 2015). However, some studies have indicated zwitterionic coatings may offer superior resistance to nonspecific binding (Jiang & Cao, 2010), perhaps leading to enhanced circulation times and increased tumor accumulation (Romberg et al., 2007). A supporting study was performed by Liu et al. who compared PEGylated and zwitterionic gold particles in terms of blood circulation and tumor accumulation (Liu et al., 2014). The zwitterionic particles were observed to have circulation half-lives almost five times greater than that of PEGylated particles in addition to tumor concentrations twice as large. A conflicting result was reported by Frellsen et al. who observed greater circulation half-lives using PEG coatings compared to zwitterionic coatings (Frellsen et al., 2016). Whether PEG or a zwitterion will perform better will depend on the molecular weight of the PEG and the type of zwitterionic coating that is used.

In addition to relying on the EPR effect, active targeting ligands are commonly attached to the surface of both therapeutic and imaging agents in efforts to further increase concentrations within tumor tissues (Byrne, Betancourt, & Brannon-Peppas, 2008; Lammers, Hennink, & Storm, 2008). Various types of targeting agents have been used in nanomedicine including small molecules (Bhattacharya et al., 2007; Wang et al., 2013b), peptides (Arosio, Manzoni, Araldi, & Scolastico, 2011; Yin, Mai, Gan, & Chen, 2014), antibodies (Chattopadhyay et al., 2012; Nakagawa et al., 2016), and nucleic acids (Dam et al., 2015; Jensen et al., 2013). However, the ability of actively targeted nanoparticles to accumulate within tumors to a greater extent than their passively (EPR effect only) targeted counterparts is currently under debate (Farokhzad & Langer, 2009; Pirollo & Chang, 2008). An early study on how targeting agents change nanoparticle interactions within tumors in vivo was performed by Choi et al. (Choi, Alabi, Webster, & Davis, 2010) In their study, the authors found that adding targeting groups to the surface of nanoparticles did little to enhance maximal concentrations within tumors. The authors did, however, observe a benefit of increased cellular internalization of particles by the tumor cells when using actively targeted particles. Another benefit of active targeting is that it can increase the retention time of nanoparticles within tumors. Qian et al. found that though targeted and nontargeted particles had similar levels of maximal concentrations within tumors, targeted particles maintained their concentration levels over a longer period of time (Qian et al., 2007). Significant decreases in nontargeted particles were noticed within a few hours. Similar results were observed by Dinesh et al. where actively targeted particles extended tumor residence times to periods of days, whereas passively targeted counterparts left tumor sites within 4–6 hrs (Dinish, Balasundaram, Chang, & Olivo, 2015). Some studies have even observed targeted particles having deeper penetration within tumors (Lane, Qian, Smith, & Nie, 2015; Lu et al., 2012). In this case particles traverse through densely packed cancer cells by a series of endocytotic and exocytotic events. An undesirable effect when using active targeting is that particles become more prone to nonspecific binding and will therefore display shorter circulation times and increased uptake within RES organs. For instance, Huang et al. examined the differences in circulation, biodistribution, and tumor uptake between active and passively targeted gold nanorods (Huang et al., 2010). In this study they observed that active targeting decreased the circulation half-lives of

nanoparticles 30–50%, and increased the concentrations that localized to the liver and spleen. Thus, when using active targeting one must weigh the benefits of the increased residence time and cellular internalization within tumors to that of the increased RES uptake. Increased residence times and cellular internalization are highly desired in therapeutic applications but increasing concentrations to RES organs at quicker rates may induce greater toxic responses.

4.2 | Size

At small molecular size scales, therapeutic and imaging agents are able to diffuse freely through tumor tissues but are also cleared out quickly and have significant widespread distributions within normal tissues (Lane, Qian, Smith, & Nie, 2015; Matsumura & Maeda, 1986). Particles reaching into the micron size scale are unable to permeate through the fenestrations of abnormal tumor vasculatures having pore cut-off sizes of a few hundred nanometers (Jain & Stylianopoulos, 2010). To take advantage of the abnormal tumor pathology leading to the EPR effect requires particles to have nanometer sizes. Within the nanometer range, significant differences in the tumor accumulation and residence time can be altered through changes in the size of the particle. Additionally, size plays an important role in how far the particles are able to penetrate into tumors. Tumors are densely packed with cells and extracellular matrices (Chauhan, Stylianopoulos, Boucher, & Jain, 2011; Jain, 2013; Jain & Stylianopoulos, 2010; Stylianopoulos & Jain, 2015). As diffusion scales inversely with size, larger particles may not be able to move beyond the tumor periphery once extravasated. For therapy, deep tumor penetration may be necessary for effective treatment as all cancer cells must be reached (Cabral et al., 2011; Chauhan et al., 2012; Li et al., 2016a; Wong et al., 2011; Zhang et al., 2018). On the other hand, for imaging applications, remaining at the tumor periphery may be sufficient as particles mark the border between normal and diseased tissues.

An early study examining size effects of gold nanoparticles localizing to tumors was performed by Perrault et al. (Perrault, Walkey, Jennings, Fischer, & Chan, 2009) Using particles within the size range of 20–100 nm they found that smaller particles were able to diffuse deeper within tumor tissues from the vasculature; however, larger particles were found to have greater overall accumulation within tumors. The lower accumulation of the 20 nm particles was deemed to be a result of a less-dense PEG layer leading to lower circulation half-lives. Later studies with PEGylated gold particles found that smaller particles tend to have longer circulation times than larger particles. Chou and Chan found that smaller particles in the size range of 15–100 nm will have longer circulation times at any given chain length of PEG coating (Chou & Chan, 2012). For instance, Chou and Chan found that 15 nm particles had circulation half-lives that were 4.4 times longer than 100 nm particles with similar PEG coatings. Similarly, Zhang et al. found that 20-nm PEGylated particles had longer circulation times than 80 nm particles (Zhang et al., 2009). With more particles remaining in the blood circulation, it is possible to have a greater driving force for particles to accumulate within tumors. Huang et al. found that smaller particles not only had greater tumor penetration but also higher accumulation as well (Huang et al., 2012). Here they compared gold particles with core sizes of 2, 6, and 15 nm with tiopronin coatings. The 2 nm particles had nearly four and seven times the tumor concentration after 24 hrs compared to 6 and 15 nm particles, respectively. The authors also found that the 2 and 6 nm particles had markedly greater perfusion throughout the entire tumor whereas the 15 nm particles tended to remain at the tumor periphery near the blood vessels.

Size can also impact the tumor accumulation of actively targeted nanoparticles. A study examining how size can impact the targeting function of nanoparticles toward tumors was performed by Sykes et al. (Sykes, Chen, Zheng, & Chan, 2014). The authors found that when particles are at sizes within 30–60 nm, active targeting can aid in increasing particle accumulation within tumors over passive targeting. Active targeting can offer particles within this size range near twice the maximal accumulation over passively targeted counterparts. Only slight increases in the accumulation were observed when targeting ligands were added to particles of smaller (15 nm) and larger (100 nm) sizes. For large particles, targeting may be unnecessary. Once large particles have extravasated from the tumor vasculature, they are less likely to diffuse into or away from the tumor periphery. Therefore, adding affinity toward the cancer cells will do little to keep particles at the tumor site. Small particles on the other hand can be aided by active targeting. Affinity toward cancer cells can prevent extravasated particles reentering the blood stream after blood concentrations have been depleted. However, active targeting can also diminish small particles ability to diffuse into tumor tissues, an effect called the "binding site barrier" (Lane, Qian, Smith, & Nie, 2015; Miao et al., 2016; Saga et al., 1995). Particles in the 30–60 nm size range can benefit from the affinity toward cancer cells to maintain particles at the tumor site and by being at size ranges more efficiently internalized by cells (Gao et al., 2005; Zhang, Li, et al., 2009). Efficient cellular internalization can increase the concentration gradient from the blood vessel to the tumor, thereby allowing more particles to enter.

Zheng et al. have shown that particles of only a few nanometers in size can still exhibit an EPR effect and accumulate to tumors at greater levels than small molecular dyes (Liu et al., 2013b). Here they demonstrated 2.5 nm glutathione-coated gold particles have similar physiological stability and renal clearance compared to small organic dyes, but the nanoparticles had longer tumor retention times and faster normal tissue clearance. The dye examined had short normal and tumor tissue half-lives of 2.3 and 1.4 hrs, respectively. The gold nanoparticles on the other hand had 90% of its maximum tumor concentration

remain up to 24 hrs after the injection and more than 90% of the concentration within the normal tissues was cleared within 44 min. Further improvements were made when the gold clusters were coated with PEG instead of glutathione. PEGylated particles had tumor targeting efficiencies three times greater than the glutathione-coated counterparts while maintaining similar normal tissue clearance rates (Liu et al., 2013c). Though achieving greater maximal concentrations at the tumor site, PEGy-lated particles had slower tumor accumulation rates. In imaging applications, slower tumor accumulation rates can increase the time required to achieve a desired contrast between tumor and normal tissues.

4.3 | Shape

Anisotropic particles have recently garnered great interest for tumor imaging and therapy (Decuzzi, Pasqualini, Arap, & Fer-rari, 2008; Kinnear, Moore, Rodriguez-Lorenzo, Rothen-Rutishauser, & Petri-Fink, 2017; Toy, Peiris, Ghaghada, & Karatha-nasis, 2014). This interest resulted from observations of anisotropic particles to be better at avoiding nonspecific uptake and have greater tissue diffusion rates than similarly sized spherical counterparts (Doshi et al., 2010; Doshi & Mitragotri, 2010; Kersey, Merkel, Perry, Napier, & Desimone, 2012; Stylianopoulos & Jain, 2015; Tan, Shah, Thomas, Ouyang, & Liu, 2013; Venkataraman et al., 2011; Zhang, Fang, Chen, Taylor, & Wooley, 2008). The combination of these effects can lead to pro-longed circulation half-lives and greater tumor accumulation. A study examining how particle shape can influence the tumor accumulation of particles was performed by Black et al. (Black et al., 2014) In this work, the authors compared gold particles having shapes of spheres, rods, discs and cubical cages. All samples tested had similar sizes of 50 nm and PEG coatings. At 24 hrs after injection, spherical particles had near 10, 6, and 3 times the tumor concentration compared to rods, discs, and cages, respectively. However, rods and cages had better perfusion of particles throughout the whole tumor, whereas spheres and disks mainly remained at the tumor periphery. The cubical cages having greater perfusion within tumors is an interesting result as they do not have the smaller cross-sectional dimensions that rods exhibit. The authors explained this result due to the increased buoyancy of the less dense hollow cages being less susceptible to increased interstitial fluid pressures within tumors. On the other hand, Tang et al. found that for small gold particles less than 3 nm, that increasing density favored greater particle margination within the blood vessels and greater overall tumor accumulation (Tang et al., 2016). By incorporating silver into the gold core to lower the overall density of the particle, the tumor accumulation decreased linearly with decreasing density. When the cores reached pure silver, which has a density about half that of gold, the tumor accumulation is reduced almost fivefold. Therefore, there may be a balance between vessel margination efficiency and buoyancy to increase tumor uptake of particles by modifying density. Results showing nanorods having more accumulation within tumors over spheres was reported in a previous study carried out by Arnida et al. (Arnida et al., 2011) Here they compared rods of dimensions 10 × 45 nm to spheres of 50 nm, both with PEG coatings. The nanorods had nearly six times the concentration within tumors over spheres. In their study the authors also found that the rods had less protein adsorption, less macrophage uptake, and longer circulation half-lives. All of these effects combined promote greater uptake into tumor tissues. The conflicting results between studies may be a result of different aspect ratios and volumes of the nanorod samples used in the comparisons. Liu et al. performed a comparison between 50 nm-sized spheres, disks, and rings (Liu et al., 2017). The authors found that the rings had around 1.5 times higher tumor accumulation than the disks and spheres which both accumulated at similar levels. Moreover, the rings also had greater tumor perfusion followed by the disks then the spheres. The authors attributed the greater perfusion as a result of the rings being hollow in the center and having a smaller dimension promoting quicker diffusion rates. Tong et al. showed that circulation half-lives, tumor accumulation, and tumor perfusion depends heavily on the aspect ratio (smaller dimension/longer dimension) and overall volume of nanoparticles (Tong et al., 2016). Here they used gold nanorods having dimensions of 2 × 10, 10 × 37, 13 × 40, 13 × 70, and 18 × 45 nm. The authors found that longer circulation half-lives can be achieved by using particles with smaller volumes. This may be the result of smaller particles having less surface area and affinity for opso-nization. The authors also observed that tumor accumulation correlated with the aspect ratio of the particles. Particle concen-trations within tumors had a linear relationship that increased as the aspect ratio of the particle increased. Interestingly, the overall particle volume had little influence over this relationship. In addition to avoiding nonspecific cellular uptake, aniso-tropic particles with greater aspect ratios, such as nanorods, may lead to higher tumor accumulation as a result of greater blood vessel margination. When particles have greater concentrations at the vessel margins as they flow through the blood, more par-ticles are available to cross the leaky vasculature at the tumor site. Previous mathematical simulations have shown that parti-cles with greater aspect ratios experience greater lateral drifts away from the centerline of a blood vessel (Di Carlo, Irimia, Tompkins, & Toner, 2007; Sei-Young, Mauro, & Paolo, 2009). In an experimental study conducted by Toy et al. (Toy, Hayden, Shoup, Baskaran, & Karathanasis, 2011), they observed that nanorods having an aspect ratio near 2 (size of 25 × 56 nm) had near eight times the concentration at vessel walls than 60 nm spheres. Whether there are linear increases in con-centration at the vessel margins with increasing aspect ratio has yet to be determined (Figure 4).
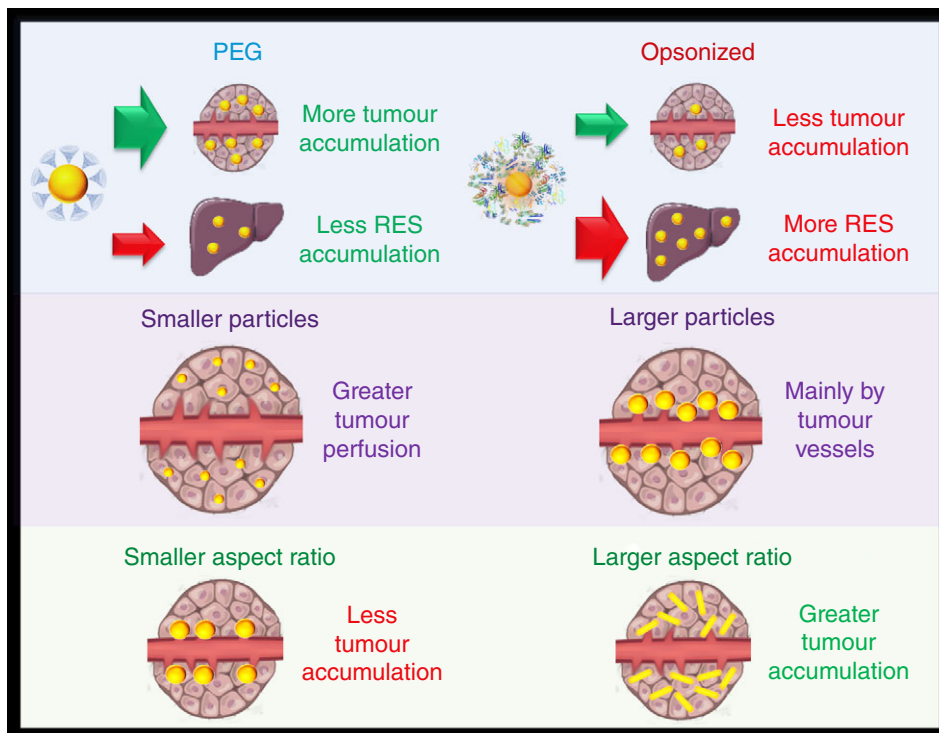
FIGURE 4 Particles with coatings that prevent nonspecific binding like PEG have greater tumor accumulation and less RES organ accumulation than particles that have been opsonized. Smaller-sized nanoparticles tend to have greater tumor perfusion whereas larger particles tend to remain at the periphery near the vessel. This is due to the greater diffusivity of smaller particles through tissues. Particles with greater aspect ratios are seen to have higher tumor accumulation than more spherical-shaped counterparts. The enhancement is believed to be a result of having greater diffusivity within tissues and having greater margination toward the vessel walls when in circulation

5 | ELIMINATION

Nanoparticles are eliminated from the body through a combination of renal and hepatobiliary pathways (Tianmeng et al., 2014; Yu & Zheng, 2015; Zhang, Poon, Tavares, Mcgilvray, & Chan, 2016). In the hepatobiliary pathway, particles accumulated within the liver are processed by hepatocytes and excreted into the bile for subsequent elimination within the feces (Longmire, Choyke, & Kobayashi, 2008). In the renal pathway, particles must be small enough to pass through the glomerular filtration of the kidneys (Yu & Zheng, 2015). Particles passing this threshold will then move on to the bladder for eventual elimination via urine excretion. Efficient clearance is of particular significance for nanoparticles that are used for imaging purposes. To obtain clinical approval, it is necessary that all foreign material originating from nanoparticles be eliminated from the body in a reasonable timeframe (Choi et al., 2007). After an imaging application has been performed, there is no purpose for any imaging material composed of foreign materials to remain within the body, even if the material is deemed nontoxic. Though drug delivery particles are designed to have long circulation times and are desired to avoid quick clearance, it is still important that they are also comprised of materials that can be eliminated after their drug payloads have been depleted. The renal pathway is the quickest route of elimination for particles where significant portions of the injected dose can be eliminated from the body within the first few hours after injection (Yu & Zheng, 2015). The hepatobiliary pathway takes a much longer time where clearance is prolonged to months or even years (Khlebtsov & Dykman, 2011; Longmire et al., 2008; Sadauskas et al., 2009). The size, shape, and surface chemistry of a particle have significant control over which pathway is chosen for elimination and its efficiency to be excreted by that pathway.

5.1 | Surface chemistry

The surface chemistry, even for particles that are small enough to enter the renal pathway, plays a substantial role in the clearance efficiency of particles. For the kidney, the glomerular passages have a negative surface charge which can affect how charged particles move through this system (Vinluan III & Zheng, 2015). Another effect is that if the particles are prone to opsonization, the protein corona can lead to a particle that was once at a size small enough for renal filtration is no longer able to pass. The liver as an organ of the RES has specialized macrophage cells, called Kupffer cells, which are responsible for most of the elimination of particles captured by the RES (Bertrand & Leroux, 2012). Like other macrophages of the RES, Kupffer cell internalization efficiency depends on the surface chemistry of the particle. Particles that are prone to opsonization

have high accumulation within the liver (Zhang et al., 2016), most of which will reside within the Kupffer cells. Particles that are captured by Kupffer cells tend to remain internalized, leading to prolonged excretion times (Zhang et al., 2016). Though particles that have surface chemistries resisting nonspecific binding may still experience high liver accumulation if renal clearance is not favored. However, it is possible that these particles have a greater chance to be processed by hepatocytes rather than Kupffer macrophages. The hepatobiliary clearance pathway involves endocytosis of matter by hepatocytes which process internalized materials and excrete them into the bile at the biliary system (Longmire et al., 2008; Tsoi et al., 2016). Therefore it is important that particles avoid Kupffer cell sequestration in order to clear via the bile in an efficient manner (Zhang et al., 2016).

For 3 nm particles, Wang et al. found that particles with anionic coatings had less renal clearance than particles with either cationic or zwitterionic coatings (Wang et al., 2016). Anionic particles tended to have greater RES uptake and located to the liver in greater amounts than the other particles studied. The cationic particles had higher accumulation within the kidneys than the neutral particles indicating that they have slightly higher renal clearance rates, but the cationic particles also had greater retention within the liver. This supports the idea that coatings that are less prone to nonspecific binding can lead to a greater over all clearance rate from the body when both the renal and hepatobiliary pathways are considered. Lipka et al. compared the excretion of 5 nm gold particles with coatings of either small anionic molecules or PEG (Lipka et al., 2010). Both particles had little clearance by the renal pathway; however, the PEG-coated particles had almost an order of magnitude increase in the administered mass cleared by the hepatobiliary pathway with 6.5% of the administered dose eliminated at 24 hrs. Gazeau et al. compared the elimination of anionic micelle-like coatings to that of PEG coatings on 13 nm particle cores (Kolosnjaj-Tabi et al., 2015). Since both particles are too large for efficient renal filtration, their excretion relied heavily upon hepatobiliary clearance. The anionic micelle-coated particles had twice the overall liver accumulation within the first day compared to the PEGylated particles, and near 15% of the injected dose remained within the liver for a year. These observations are perhaps a result of the anionic particles being quickly removed from the blood into the liver by the Kupffer macrophages which retain the particles over long periods of time. The PEGylated particles were able to clear out of the liver to undetectable levels within a year's time.

PEG, though allowing more efficient hepatobiliary clearance, may increase the HD of particles too much to be efficiently cleared via renal filtration. However, if the cores of the particles are small enough, a PEG coating can still be applied and renal clearance may be maintained (Liu et al., 2013c; Zhang et al., 2015). To increase renal clearance of small nanoparticles, zwitterionic coatings are a preferable choice. Many zwitterionic coatings add little thickness to the overall HD of the particle while still preventing nonspecific binding of proteins and cells. Zheng et al. have used zwitterionic glutathione for small renal clearable gold particles (Yu, Zhou, Liu, Hankins, & Zheng, 2011; Zhou, Long, Qin, Sun, & Zheng, 2011). Glutathione is a small peptide that has low affinity toward proteins in the blood (Hong et al., 2006). The group was able to demonstrate that gold cores of 1.7 and 2.5 nm when capped with glutathione led to HDs of 2.1 and 3.3 nm, respectively. Since the glutathione coatings were able to resist protein adsorption and had small sizes, the particles had clearances greater than 50% of the injected dose within a 48-hr period. These clearance rates were noted to be 10–100 times that of similarly sized particles with anionic coatings. Other zwitterionic ligands such as dithiolated-polyaminocarboxylate (DTDTPA) have also been shown to be good coatings for renal clearable small gold particles (Alric et al., 2013). In the case of DTDTPA, particles that had a 2.4 nm core and a HD of 6.6 nm were able to achieve 64% clearance of the injected dose within a 24-hr period. We note that not all zwitterions will allow small particles to clear the renal system. Zhou et al. found that 2–4 nm gold particles coated with cysteine, though stable in water, aggregated into structures that were larger than 100 nm when encountered with biological fluids (Zhou et al., 2011). They also observed near 55% of an injected dose accumulates to the liver, likely being aggregates too large to pass the renal pathway.

5.2 | Size

The hydrodynamic size of the nanoparticle has the strongest influence on whether the nanoparticle is able to pass through the renal pathway, where particles typically need to have HDs less than 10 nm to pass (Burns et al., 2009; Chen et al., 2014b; Huang et al., 2013; Longmire et al., 2008; Choi et al., 2007; Tang, Chen, & Zheng, 2014; Yang et al., 2015). This threshold is set by the size glomerular pores inside the kidney that filter the blood plasma. Particles that are larger than the glomerular pore sizes will rely heavily upon the hepatobiliary pathway for clearance, which is significantly slower than the renal pathway. In addition to determining which pathway is chosen for excretion, size also plays a role in how efficiently the particles are excreted by each pathway.

An early study examining the effect of size on the clearance of gold nanoparticles via both excretion pathways was carried out by Brandau et al. (Semmler-Behnke et al., 2008) Here they examined the excretion differences between 1.4 and 18 nm gold particles having coatings of triphenylphosphine sulfonate. The 18-nm particles had nondetectable levels within the urine at 24 hrs, most likely as a result of being too large to pass through kidney filtration. Almost the entirety of the injected dose

located to the liver with only 0.5% of the injected dose excreted by the hepatobiliary pathway in a 24-hr period. The smaller 1.4 nm particles had more efficient excretion by both pathways with near 9% leaving within the urine and 5% leaving within the feces in a 24-hr period. Balogh et al. also found enhanced excretion in both pathways with smaller particles when comparing 5 and 22 nm poly(amidoamine) dendrimer gold constructs (Balogh et al., 2007). Here they found that the 5 nm particles had 18% of the injected dose cleared by urine within 24 hrs with 1.4% cleared by the feces. The 22 nm particles had 11% clearance by urine and 0.75% cleared by feces in the same time period. Zhou et al. observed an exponential increase in the renal clearance of particles as the sizes decreased (Zhou et al., 2011). Here glutathione-coated particles with HDs of 2, 6, and 13 nm had renal clearance efficiencies of 50%, 4%, and 0.5% of the injected dose in 24 hrs, respectively. It is important to note that the clearance efficiency depends on the hydrodynamic size of the nanoparticle which includes the thickness of the coating plus the size of the core. Zhao et al. demonstrated this in their work comparing the clearance of 2.5 nm particles having either 350 or 1,000 molecular weight PEG coatings (Zhao, Sultan, Detering, Luehmann, & Liu, 2014). The 350 and 1,000 molecular weight PEG coatings led to hydrodynamic sizes of 4.3 and 6.9 nm, respectively. The 4.3 nm-sized particles had 31.4% of the injected dose clearing within the urine in a 24-hr period compared to 6.73% clearance of the 6.9 nm particles. The 6.9 nm particles did have a slightly higher percentage of the injected dose cleared by the hepatobiliary system than the 4.3 nm particles being 34 and 26.5%, respectively. This result is in part due to less of the smaller particles locating to the liver by having much greater renal clearance. When combining both pathways, the clearance of the injected dose of the 4.3 nm particles was nearly 50% greater than that of the 6.9 nm despite the small difference in hydrodynamic size. Interestingly, as particles get as small as 1 nm, reduction in renal filtration is observed with smaller particle sizes (Du et al., 2017). Du et al. using small gold particles consisting of 25, 18, 15, and 10 atoms, found an exponential decrease in the glomerular filtration of particles as the number of atoms decreased (Du et al., 2017). At 24 hrs post injection, the urinary excretion for the 25, 18, 15, and 10 atom particles was observed to be 51.57, 26.82, 22.90, and 19.07% of the injected dose, respectively. The decrease in the ability of the smaller-sized particles in this size regime to clear the renal system was attributed to increased interactions with the glomerular glycocalyx. The glycocalyx potentially has pores of sizes around 1 nm, thus smaller particles will have greater penetration into these pores leading to longer retention times similar to what is observed in size-exclusion chromatography.

Larger particles that are in the tens of nanometers are commonly observed to have marginal or no excretion at all by the renal pathway, thus leaving their clearance dominated by the hepatobiliary pathway (Yu & Zheng, 2015; Zhang et al., 2016). Generally the excretion time for these larger-sized particles is significantly longer than those having sizes <20 nm. Sadauskas et al. found that 40 nm citrate-coated particles accumulated mostly to the Kupffer cells of the liver, with only a 9% decrease in the amount located to the liver 6 months post injection (Sadauskas et al., 2009). However, citrate-coated nanoparticles tend to be unstable in biological fluids, being opsonized and aggregating into larger constructs, thus exacerbating their inefficient excretion. On the other hand, it is possible to have larger particles cleared more quickly through the hepatobiliary system if they have a coating which prevents opsonization and prolonged macrophage sequestration. You et al. observed that 63 nm PEGylated gold particles had 28.6% of the liver content excreted within a period of 90 days (You et al., 2014). PEGylated particles of sizes near 120 nm have been found to have their liver levels decrease over 30% within a 2-week timeframe post injection (Thakor et al.,). We acknowledge that the prolonged excretion of larger gold nanoparticles can also be in part to the inert chemical nature of the inorganic core. Therefore, there is no efficient mechanism to break down large gold particles into smaller parts for more efficient excretion. However, large particles made of materials that can be degraded by cells, also show hepatobiliary clearance periods lasting several months (Gu, Fang, Sailor, & Park, 2012; Kumar et al., 2010; Sun, Feng, Yang, Huang, & Li, 2015). We note that many clearance studies of nanoparticles have been performed on rodent species. Rodents can exhibit accelerated hepatobiliary clearances compared to humans and particles that are larger than the renal threshold may require metabolic breakdown into smaller constituents to efficiently leave the body (Bulte et al., 2014).

5.3 | Shape

In addition to the size controlling whether a particle can be cleared by the renal system, shape can also be used as a method to aid renal passage of particles having a dimension that may be larger than the pore sizes of the glomerulus. Theoretical calculations have previously shown rod-shaped particles with a cross-sectional diameter less than the size of the glomerular pores can have the ability to be cleared by the renal system, despite having lengths significantly greater in size (Ruggiero et al., 2010). Smaller cross-sectional diameters may also lead to increased hepatobiliary clearance as well. Experimental results by Li et al. showed that gold nanorods with cross-sectional diameters at sizes less than the 10 nm glomerular threshold had efficient clearance from the body, whereas those with larger cross-sectional diameters do not (Li et al., 2016b). Here they compared the elimination of nanorods with dimensions of 7 × 30 nm and 14 × 56 nm. The smaller rods that had located to the kidney and liver had only 2–3% of the initial measured values remaining after a 30-day period. The larger rods, however, had 40–50% of the initial accumulations remaining within these organs over the same time period. The percentage of the injected dose remaining within the entire body after the 30-day period was 0.68 and 12.3% for the 7 × 30 nm and 14 × 56 nm rods, respectively.

Conflicting results were observed by Ali et al. who examined the long-term fate of gold nanorods having sizes of 25×5.5 nm and 72×16 nm (Ali et al., 2017). Their results found little clearance of the particles from the liver and kidney during the entirety of the study. A potential explanation for the differences in results is that these particles had different thicknesses in coatings. The study by Li et al. had albumin coatings which add a thickness of a few nanometers. El-Sayed et al. used 10,000 molecular weight PEG coatings which can add over a 10-nm thick layer to the particle. Interestingly in a study by Ye et al., they observed large gold nanotubes of 75 nm diameters and 300–525 nm lengths having complete elimination from the body in a period of 72 hrs (Ye et al., 2015). In addition to having no dimension small enough to fit through glomerular pores, the nanotubes had highly negatively charged coatings which can also impede efficient renal clearance. If relying on solely the hepatobiliary pathway, such clearance efficiency is impressive. The mechanism for such efficient clearance of these particles, whether mainly from the renal or hepatobiliary pathway, needs deeper exploration. Nevertheless, rod-shaped particles that are able to clear the renal system offer an opportunity to load more imaging or therapeutic agents as they have greater volumes and surface areas than would spheres that can pass through similar pore sizes.

Talamini et al. examined the differences in excretion between 50 nm spheres, 60×30 nm rods, and 55 nm stars (Talamini et al., 2017). In this study, all particles were coated with small molecular weight PEG ligands to minimize hydrodynamic size and aspect ratio changes (Tay, Setyawati, Xie, Parak, & Leong, 2014). Within a 120-hr period after injection, 20% of the injected dose of rods remained within the body whereas the stars and spheres had similar retention levels of 60–80% of the injected dose remaining. The levels of particles measured in the kidney and liver soon after injection and 120 hrs post injection had similar levels for the stars and spheres, with little of the injected dose able to clear out of these organs through the urine or feces. The rods showed a slow steady decline in both organs within this same time period. Gold stars have spikey protrusions that have high aspect ratios and small cross-sections, but these protrusions sick out in all directions leaving the particle with an overall cross-section that would be similar to a sphere. Therefore, both spheres and stars would be expected to have similar behaviors for kidney clearance. On the other hand, the authors found that the stars had greater retention within the Kupffer cells of the liver. It may be possible that the protrusions of stars enhance cellular uptake by these macrophages, possibly resulting in noticeable clearance differences between the stars and spheres if the study was conducted over a longer time period (Figure 5).

6 | NEXT GENERATION DESIGNS TO OVERCOME BARRIERS

In addition to the pathological features of tumors including leaky vasculature and impaired lymphatics leading to the EPR effect, tumors also exhibit abnormal levels of enzymes and acidic environments (Balkwill, Capasso, & Hagemann, 2012; Kato et al., 2013; Kessenbrock, Plaks, & Werb, 2010). Next generation designs of nanoparticles take advantage of these cues to further enhance the delivery and retention of particles within diseased tissues. Here we consider two design concepts for next generation particles, smaller particles that assemble into larger structures at tumor sites, and larger particles that disassemble into smaller particles at tumor sites. Smaller particles assembling into larger constructs are a design we deem more suitable for imaging applications. This design allows small particles to quickly locate and assemble within the tumor leading to their long-term retention, while the nonassembling particles within the normal tissues are quickly cleared from the body. This process can create large contrast ratios (tumor signal to normal tissue signal) in short timeframes and decrease toxicity concerns of chronic exposure to the contrast agent. Larger constructs that disassemble into smaller particles is a design we deem more suitable for drug delivery. The larger construct can maintain longer circulation times by avoiding quick blood clearance and have a strong EPR effect to increase tumor accumulation. Once at the tumor site, the larger constructs disassemble into smaller particles which permeate deeper into the diseased tissue. This concept can allow treatment of cancer cells throughout the entire tumor at higher concentrations. Also, particles that do not end up at the tumor site can still be efficiently broken down and eliminated more quickly. Here we provide a few representative examples demonstrating these concepts using gold nanoparticles.

6.1 | Small particles assembling into large particles

Ruan et al. used an assembly method that relies on the presence of acidic pH and legumain (Ruan et al., 2016). Legumain is an enzyme that is overexpressed in several cancers. In this case the pH and legumain-exposed moieties that can covalently link particles together by a click cycloaddition reaction. Here particles of 20 nm size entering the tumor microenvironment assembled into structures having sizes near 300 nm. The authors found that the assembly mechanism more than doubled the number of particles that were retained within tumors. The particles that assembled into larger structures had 7.52% of the injected dose localize to the tumor in a 24-hr period whereas counterparts lacking functional groups for assembly had 3%. Gao et al. used a similar design to have gold particles give stronger optical signals when imaging tumors (Gao et al., 2017). Though we note
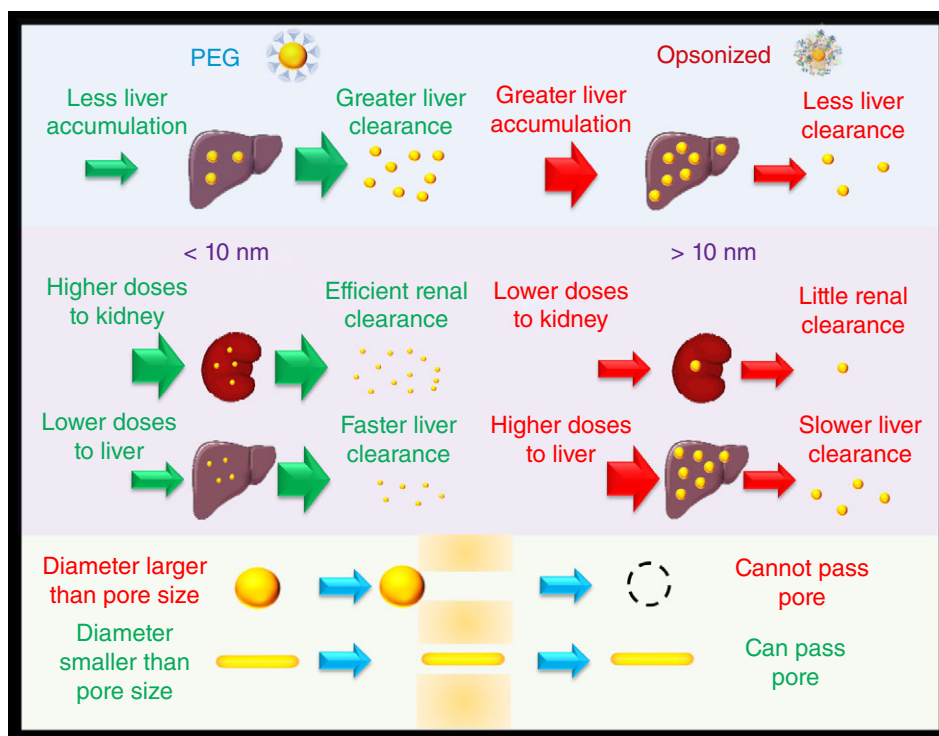
FIGURE 5 Particles having coatings that resist nonspecific binding like PEG not only have less accumulation within the liver, but the particles that do accumulate have quicker clearance from the organ when compared to opsonized particles. Particles that are less than 10 nm in size tend to have greater amounts of the injected dose go through efficient renal clearance and less accumulate within the liver. Moreover, the particles that do accumulate in the liver have quicker clearance rates than larger-sized particles. Therefore, smaller particles tend to have a greater clearance rate overall from the body than larger-sized counterparts. Particles that are greater than 10 nm in size have little to no renal clearance and rely heavily on hepatobiliary clearance, which is a significantly slower process. Rod-shaped particles offer the ability to clear the renal system despite having a length greater than the glomerular pore size. Even with lengths significantly larger than the pore size, as long as the diameter of the rod is smaller than the pore there is a possibility for clearance. Spherical-shaped particles having diameters larger than the pore size are excluded from passing. Rod-shaped particles that are able to clear the renal system offer an opportunity to load more imaging or therapeutic agents as they have greater volumes and surface areas than would spheres that can pass through similar pore sizes

that the elimination kinetics of these particles still needs investigation as both studies used 20 nm particles, which are presumed to have slower normal tissue clearance and slower elimination from the body. Whether this technique can significantly enhance tumor accumulation of nanoparticles at sizes that can be efficiently cleared by the renal system has yet to be seen. This concept has been applied successfully outside using gold nanoparticles with aggregation-induced emission dyes and dots that are at sizes more suitable for efficient clearance from normal tissues (Feng & Liu, 2018; Ye et al., 2014).

6.2 | Large particles disassembling into small particles

Chou et al. developed superstructures constructed of small gold nanoparticles linked together by DNA which were observed to have high tumor accumulation and increased clearance properties (Chou, Zagorovsky, & Chan, 2014). The superstructures consisted of a 13-nm particle core that was functionalized with DNA and satellite particles of 3 nm were linked to the core via complimentary DNA strands. To increase the stability of the superstructures, the satellite particles were coated with 1 kDa PEG. The superstructures had greater resistance to nonspecific uptake by macrophages as the number of satellite particles was increased. The superstructures that did have uptake by macrophages broke down to smaller particles that were exocytosed from the cell. Moreover, the superstructures can disassemble to let smaller particles diffuse deeper into the tissues. These properties combined can lead to significant increases in tumor accumulation. Compared to the nonassembled particles, the tumor accumulation of the superstructures had over a twofold increase in the number of particles. The superstructures also exhibited efficient renal clearance by being able to break down to 3 nm parts with 15% of the injected dose detected in the urine 48 hrs post injection. As a design for drug carriers the accelerated clearance from nontarget organs can reduce the systemic toxicity of the therapeutic. This strategy has been successfully employed to treat tumors where a 100 nm-sized polymeric particle sensitive to the acidic microenvironment of tumors could disassemble to 5-nm drug carriers (Li et al., 2016). Here superstructures were observed to have superior tumor killing properties compared to using either 100- or 5-nm drug carrying particles (Figure 6).
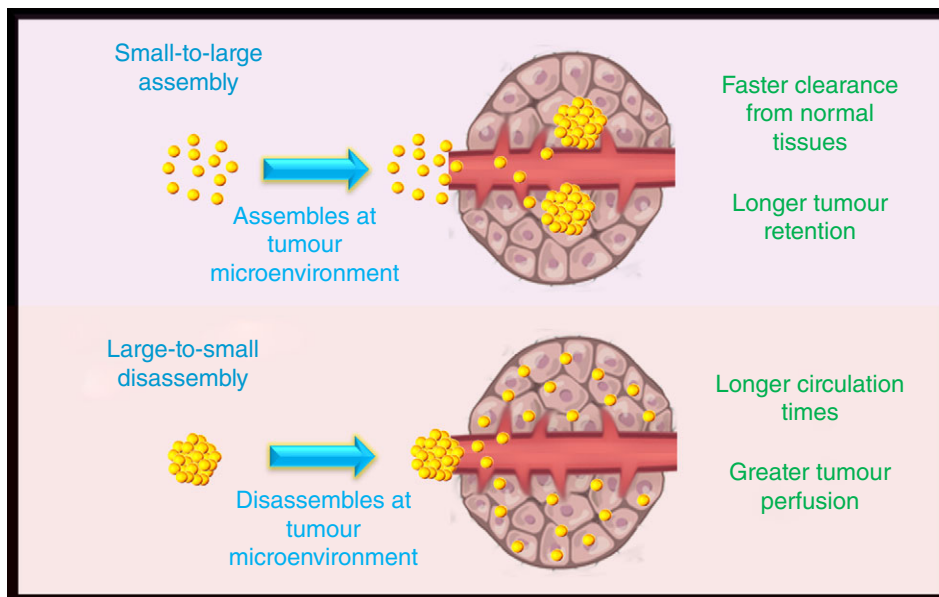
FIGURE 6 Next generation designs in nanomedicine involve particles that respond to physiological cues from the tumor microenvironment. Two such designs are small particles that assemble into larger structures at tumors (small-to-large assembly), the other is larger particles that disassemble in to smaller particles at tumors (large-to-small disassembly). The small-to-large disassembly process forms large particles at the tumor that are too large to diffuse out and therefore are retained, whereas the particles not localized to the tumor are quickly cleared from the body. The large-to-small disassembly process has large structures that have long circulation times that once at the tumor site, disassembles into small particles that have greater perfusion throughout the tumor tissue

7 | CONCLUSION

Studies using gold nanoparticles probing how size, shape, and surface chemistry changes their biological behaviors has provided significant gains to our understanding of the obstacles to nanomedicine and has revealed potential methods to overcome them. To date there are a wide variety of robust synthetic techniques that can precisely control the size and morphology of the particles. However, an area for improvement in synthetic techniques is greater control of the size dispersity of small particles. The coefficient of variation of particles tends to get larger for synthesis methods of smaller particles (1–10 nm) compared to larger particles (10–100 nm). With tight control over a size series of small gold nanoparticles the size threshold for renal clearance could be assessed with more accuracy. We also caution when comparing different sizes and shapes involving particles synthesized by different surfactants, it is important to ensure the final particles after ligand exchange procedures have similar surface chemistries. Particles with various shapes are commonly made with strongly bound cationic surfactants that limit surface exchange with other molecules such as thiolated PEG (Schulz et al., 2016; Xia et al., 2012). Particles having quasi-spherical and star-like shapes can have as-synthesized citrate coatings that are much easier replaced with thiolated PEG (Xia et al., 2012). Comparing between particles synthesized by different methods can lead to mistaking biological behaviors resulting from different surface chemistries as effects from particle size or shape. Thus, methods that can efficiently remove strongly bound as-synthesized coatings completely and allow more efficient ligand exchanges are needed in these analyses (He et al., 2018; Mehtala et al., 2014; Schulz et al., 2016). An avenue for further advancing the field of using gold nanoparticles in probing biological obstacles is to develop highly multiplexed methods that can evaluate several particle constructions in a single setting (Lane, Qian, & Nie, 2015). This would increase the throughput in determining favorable qualities of nanoparticles and provide true side-by-side comparisons of in vivo behaviors between particles of different size, shape, and surface chemistries. Another advancement needed is evaluating how the tumor model type changes which particle constructions are more favorable. For instance, the EPR effect can vary greatly among tumors types and the expression of surface markers can vary as well (Prabhakar et al., 2013). Therefore a single particle construction would unlikely be optimal in all tumor cases. Finally, we note that synthesis techniques of drug delivery vehicles and imaging agents composed of organic materials, which generally have higher chances for clinical approval, have yet to match the precise control of gold nanoparticle synthesis methods. Researchers are beginning to develop nanoparticles composed of organic materials that display a wide variety of shapes and sizes that potentially can emulate in vivo studies using gold nanoparticles (Meyer & Green, 2016). With the rapidly growing field of nanoparticle synthesis, organic constructions can match the preciseness of gold in the near future. However, we feel gold nanoparticles will still remain as model systems due to their chemical and physical properties allowing for highly sensitive and specific detection which are essential in accurately assessing biological behaviors of nanomedicines.

ACKNOWLEDGMENTS

CONFLICT OF INTEREST

The authors have declared no conflicts of interest for this article.

RELATED WIREs ARTICLES

ORCID

Lucas A. Lane https://orcid.org/0000-0002-1464-8866

REFERENCES

Acres, R. G., Feyer, V., Tsud, N., Carlino, E., & Prince, K. C. (2014). Mechanisms of aggregation of cysteine functionalized gold nanoparticles. *The Journal of Physical Chemistry C*, *118*, 10481–10487. https://doi.org/10.1021/jp502401w

Ajdari, N., Vyas, C., Bogan, S. L., Lwaleed, B. A., & Cousins, B. G. (2017). Gold nanoparticle interactions in human blood: A model evaluation. *Nanomedicine: Nanotechnology, Biology and Medicine*, *13*, 1531–1542. https://doi.org/10.1016/j.nano.2017.01.019

Akinc, A., & Battaglia, G. (2013). Exploiting endocytosis for nanomedicines. *Cold Spring Harbor Perspectives in Biology*, *5*, a016980. https://doi.org/10.1101/cshperspect.a016980

Albanese, A., Tang, P. S., & Chan, W. C. W. (2012). The effect of nanoparticle size, shape, and surface chemistry on biological systems. *Annual Review of Biomedical Engineering*, *14*, 1–16.

Ali, M. R., Rahman, M. A., Wu, Y., Han, T., Peng, X., Mackey, M. A., … Mostafa, A. E. (2017). Efficacy, long-term toxicity, and mechanistic studies of gold nanorods photothermal therapy of cancer in xenograft mice. *Proceedings of the National Academy of Sciences of the United States of America*, *114*, E3110–E3118. https://doi.org/10.1073/pnas.1619302114

Alkilany, A. M., & Murphy, C. J. (2010). Toxicity and cellular uptake of gold nanoparticles: What we have learned so far? *Journal of Nanoparticle Research*, *12*, 2313–2333.

Alric, C., Miladi, I., Kryza, D., Taleb, J., Lux, F., Bazzi, R., … Olivier, T. (2013). The biodistribution of gold nanoparticles designed for renal clearance. *Nanoscale*, *5*, 5930–5939. https://doi.org/10.1039/C3NR00012E

And, A. G., & Murphy, C. J. (2004). Seed-mediated synthesis of gold nanorods: Role of the size and nature of the seed. *Chemistry of Materials*, *16*, 3633–3640.

And, B. N., & Elsayed, M. A. (2003). Preparation and growth mechanism of gold Nanorods (NRs) using seed-mediated growth method. *Chemistry of Materials*, *15*, 1957–1962.

Anselmo, A. C., & Mitragotri, S. (2016). Nanoparticles in the clinic. *Bioengineering & Translational Medicine*, *1*, 10–29. https://doi.org/10.1002/btm2.10003

Antosh, M., Wijesinghe, D. D., Shrestha, S., Lanou, R., Huang, Y. H., Hasselbacher, T., … Yana, K. R. (2015). Enhancement of radiation effect on cancer cells by gold-pHLIP. *Proceedings of the National Academy of Sciences of the United States of America*, *112*, 5372–5376.

Arnedos, M., Vicier, C., Loi, S., Lefebvre, C., Michiels, S., Bonnefoi, H., & Andre, F. (2015). Precision medicine for metastatic breast cancer--limitations and solutions. *Nature Reviews. Clinical Oncology*, *12*, 693–704.

Arnida, Janát-Amsbury, M. M., Ray, A., Peterson, C. M., & Ghandehari, H. (2011). Geometry and surface characteristics of gold nanoparticles influence their biodistribution and uptake by macrophages. *European Journal of Pharmaceutics and Biopharmaceutics*, *77*, 417–423. https://doi.org/10.1016/j.ejpb.2010.11.010

Arosio, D., Manzoni, L., Araldi, E. M. V., & Scolastico, C. (2011). Cyclic RGD functionalized gold nanoparticles for tumor targeting. *Bioconjugate Chemistry*, *22*, 664–672.

Arvizo, R. R., Miranda, O. R., Moyano, D. F., Walden, C. A., Karuna, G., Resham, B., … Priyabrata, M. (2011). Modulating pharmacokinetics, tumor uptake and biodistribution by engineered nanoparticles. *PLoS One*, *6*, e24374. https://doi.org/10.1371/journal.pone.0024374

Aryal, S., Remant Bahadur, K. C., Bhattarai, N., Kim, C. K., & Kim, H. Y. (2006). Study of electrolyte induced aggregation of gold nanoparticles capped by amino acids. *Journal of Colloid and Interface Science*, *299*, 191–197. https://doi.org/10.1016/j.jcis.2006.01.045

Au, L., Zheng, D., Zhou, F., Li, Z. Y., Li, X., & Xia, Y. (2008). A quantitative study on the photothermal effect of immuno gold nanocages targeted to breast cancer cells. *ACS Nano*, *2*, 1645–1652.

Au, L., Zhang, Q., Cobley, C. M., Gidding, M., Schwartz, A. G., Chen, J., & Xia, Y. (2010). Quantifying the cellular uptake of antibody-conjugated Au nanocages by two-photon microscopy and inductively coupled plasma mass spectrometry. *ACS Nano*, *4*, 35–42. https://doi.org/10.1021/nn901392m

Balkwill, F. R., Capasso, M., & Hagemann, T. (2012). The tumor microenvironment at a glance. *Journal of Cell Science*, *125*, 5591–5596.

Balogh, L., Nigavekar, S. S., Nair, B. M., Lesniak, W., Zhang, C., Sung, L. Y., … Mamou, F. (2007). Significant effect of size on the in vivo biodistribution of gold composite nanodevices in mouse tumor models. *Nanomedicine: Nanotechnology, Biology and Medicine*, *3*, 281–296. https://doi.org/10.1016/j.nano.2007.09.001

Bartczak, D., Muskens, O. L., Nitti, S., Sanchez-Elsner, T., Millar, T. M., & Kanaras, A. G. (2012). Interactions of human endothelial cells with gold nanoparticles of different morphologies. *Small*, *8*, 122–130.

Behzadi, S., Serpooshan, V., Tao, W., Hamaly, M. A., Alkawareek, M. Y., Dreaden, E. C., … Mahmoudi, M. (2017). Cellular uptake of nanoparticles: Journey inside the cell. *Chemical Society Reviews*, 46, 4218–4244. https://doi.org/10.1039/C6CS00636A

Bertrand, N., & Leroux, J.-C. (2012). The journey of a drug-carrier in the body: An anatomo-physiological perspective. *Journal of Controlled Release*, 161, 152–163. https://doi.org/10.1016/j.jconrel.2011.09.098

Bhattacharya, R., Patra, C. R., Earl, A., Wang, S., Katarya, A., Lu, L., … Priyabrata, M. (2007). Attaching folic acid on gold nanoparticles using noncovalent interaction via different polyethylene glycol backbones and targeting of cancer cells. *Nanomedicine: Nanotechnology, Biology and Medicine*, 3, 224–238.

Black, K. C., Wang, Y., Luehmann, H. P., Cai, X., Xing, W., Pang, B., … Xia, Y. (2014). Radioactive 198Au-doped nanostructures with different shapes for in vivo analyses of their biodistribution, tumor uptake, and Intratumoral distribution. *ACS Nano*, 8, 4385–4394. https://doi.org/10.1021/nn406258m

Blanco, E., Shen, H., & Ferrari, M. (2015). Principles of nanoparticle design for overcoming biological barriers to drug delivery. *Nature Biotechnology*, 33, 941. https://doi.org/10.1038/nbt.3330

Brewer, S. H., Glomm, W. R., Johnson, M. C., Knag, M. K., & Franzen, S. (2005). Probing BSA binding to citrate-coated gold nanoparticles and surfaces. *Langmuir*, 21, 9303–9307.

Bulte, J. W. M., Schmieder, A. H., Keupp, J., Caruthers, S. D., Wickline, S. A., & Lanza, G. M. (2014). MR cholangiography demonstrates unsuspected rapid biliary clearance of nanoparticles in rodents: Implications for clinical translation. *Nanomedicine: Nanotechnology, Biology and Medicine*, 10, 1385–1388. https://doi.org/10.1016/j.nano.2014.05.001

Burns, A. A., Vider, J., Ow, H., Herz, E., Penate-Medina, O., Baumgart, M., … Bradbury, M. (2009). Fluorescent silica nanoparticles with efficient urinary excretion for nanomedicine. *Nano Letters*, 9, 442–448. https://doi.org/10.1021/nl803405h

Byrne, J. D., Betancourt, T., & Brannon-Peppas, L. (2008). Active targeting schemes for nanoparticle systems in cancer therapeutics. *Advanced Drug Delivery Reviews*, 60, 1615–1626. https://doi.org/10.1016/j.addr.2008.08.005

Cabral, H., Matsumoto, Y., Mizuno, K., Chen, Q., Murakami, M., Kimura, M., … Kataoka, K. (2011). Accumulation of sub-100 nm polymeric micelles in poorly permeable tumours depends on size. *Nature Nanotechnology*, 6, 815–823.

Caracciolo, G., Farokhzad, O. C., & Mahmoudi, M. (2017). Biological identity of nanoparticles in vivo: Clinical implications of the protein corona. *Trends in Biotechnology*, 35, 257–264. https://doi.org/10.1016/j.tibtech.2016.08.011

Cedervall, T., Lynch, I., Lindman, S., Berggård, T., Thulin, E., Nilsson, H., … Linse, S. (2007). Understanding the nanoparticle–protein corona using methods to quantify exchange rates and affinities of proteins for nanoparticles. *Proceedings of the National Academy of Sciences of the United States of America*, 104, 2050–2055. https://doi.org/10.1073/pnas.0608582104

Chakraborty, S., Joshi, P., Shanker, V., Ansari, Z. A., Singh, S. P., & Chakrabarti, P. (2011). Contrasting effect of gold nanoparticles and nanorods with different surface modifications on the structure and activity of bovine serum albumin. *Langmuir*, 27, 7722–7731.

Chandran, P., Riviere, J. E., & Monteiro-Riviere, N. A. (2017). Surface chemistry of gold nanoparticles determines the biocorona composition impacting cellular uptake, toxicity and gene expression profiles in human endothelial cells. *Nanotoxicology*, 11, 507–519. https://doi.org/10.1080/17435390.2017.1314036

Chang, H.-H., Braswell, S., George, J., Gryka, M., Kim, S., Kolmodin, N., & Pan, D. (2016). Barriers in Nanomedicine: The Importance of Defined Chemistry and Engineering Approaches for Clinical Translation. In D. Pan (Ed.), *Personalized medicine with a nanochemistry twist: Nanomedicine* (pp. 1–27). Switzerland: Springer International Publishing.

Charan, S., Sanjiv, K., Singh, N., Chien, F. C., Chen, Y. F., Nergui, N. N., … & Chen, P. (2012). Development of chitosan oligosaccharide-modified gold nanorods for in vivo targeted delivery and noninvasive imaging by NIR irradiation. *Bioconjugate Chemistry*, 23, 2173–2182. https://doi.org/10.1021/bc3001276

Chattopadhyay, N., Fonge, H., Cai, Z., Scollard, D., Lechtman, E., Done, S. J., … Reilly, R. M. (2012). Role of antibody-mediated tumor targeting and route of Administration in nanoparticle tumor accumulation in vivo. *Molecular Pharmaceutics*, 9, 2168–2179. https://doi.org/10.1021/mp300016p

Chauhan, V. P., Stylianopoulos, T., Boucher, Y., & Jain, R. K. (2011). Delivery of molecular and nanoscale medicine to tumors: Transport barriers and strategies. *Annual Review of Chemical and Biomolecular Engineering*, 2, 281–298. https://doi.org/10.1146/annurev-chembioeng-061010-114300

Chauhan, V. P., Stylianopoulos, T., Martin, J. D., Popović, Z., Chen, O., Kamoun, W. S., … Jain, R. K. (2012). Normalization of tumour blood vessels improves the delivery of nanomedicines in a size-dependent manner. *Nature Nanotechnology*, 7, 383–388.

Chen, H., Wang, G. D., Tang, W., Todd, T., Zhen, Z., Tsang, C., … Stickney, J. (2014b). Gd-encapsulated carbonaceous dots with efficient renal clearance for magnetic resonance imaging. *Advanced Materials*, 26, 6761–6766. https://doi.org/10.1002/adma.201402964

Chen, J., Saeki, F., Wiley, B. J., Cang, H., Cobb, M. J., Li, Z. Y., … Younan, X. (2005). Gold nanocages: Bioconjugation and their potential use as optical imaging contrast agents. *Nano Letters*, 5, 473–477.

Chen, L., Ji, F., Xu, Y., He, L., Mi, Y., Bao, F., … & Zhang, Q. (2014a). High-yield seedless synthesis of triangular gold nanoplates through oxidative etching. *Nano Letters*, 14, 7201–7206. https://doi.org/10.1021/nl504126u

Chen, L. C., Wang, C., Yuan, Z., & Chang, H. (2015). Fluorescent gold nanoclusters: Recent advances in sensing and imaging. *Analytical Chemistry*, 87, 216–229.

Chen, Q., Wang, H., Liu, H., Wen, S., Peng, C., Shen, M., … Shi, X. (2015). Multifunctional dendrimer-entrapped gold nanoparticles modified with RGD peptide for targeted computed tomography/magnetic resonance dual-modal imaging of tumors. *Analytical Chemistry*, 87, 3949–3956.

Chen, S., Cao, Z., & Jiang, S. (2009). Ultra-low fouling peptide surfaces derived from natural amino acids. *Biomaterials*, 30, 5892–5896. https://doi.org/10.1016/j.biomaterials.2009.07.001

Cheng, X., Tian, X., Wu, A., Li, J., Tian, J., Chong, Y., … Ge, C. (2015). Protein corona influences cellular uptake of gold nanoparticles by phagocytic and nonphagocytic cells in a size-dependent manner. *ACS Applied Materials & Interfaces*, 7, 20568–20575. https://doi.org/10.1021/acsami.5b04290

Chithrani, B. D., & Chan, W. C. W. (2007). Elucidating the mechanism of cellular uptake and removal of protein-coated gold nanoparticles of different sizes and shapes. *Nano Letters*, 7, 1542–1550. https://doi.org/10.1021/nl070363y

Chithrani, B. D., Ghazani, A. A., & Chan, W. C. W. (2006). Determining the size and shape dependence of gold nanoparticle uptake into mammalian cells. *Nano Letters*, 6, 662–668.

Cho, E. C., Au, L., Zhang, Q., & Xia, Y. (2010). The effects of size, shape, and surface functional group of gold nanostructures on their adsorption and internalization by cells. *Small*, 6, 517–522.

Cho, E. C., Liu, Y., & Xia, Y. (2010). A simple spectroscopic method for differentiating cellular uptakes of gold nanospheres and nanorods from their mixtures. *Angewandte Chemie*, 49, 1976–1980.

Cho, E. C., Xie, J., Wurm, P. A., & Xia, Y. (2009). Understanding the role of surface charges in cellular adsorption versus internalization by selectively removing gold nanoparticles on the cell surface with a I2/KI etchant. *Nano Letters*, 9, 1080–1084.

Cho, W. S., Cho, M., Jeong, J., Choi, M., Cho, H. Y., Han, B. S., … Jeong, J. (2009). Acute toxicity and pharmacokinetics of 13 nm-sized PEG-coated gold nanoparticles. *Toxicology and Applied Pharmacology*, 236, 16–24. https://doi.org/10.1016/j.taap.2008.12.023

Choi, C. H. J., Alabi, C. A., Webster, P., & Davis, M. E. (2010). Mechanism of active targeting in solid tumors with transferrin-containing gold nanoparticles. *Proceedings of the National Academy of Sciences of the United States of America*, 107, 1235–1240.

Choi, H. S., Liu, W., Misra, P., Tanaka, E., Zimmer, J. P., Ipe, B. I., … Frangioni, J. V. (2007). Renal clearance of quantum dots. *Nature Biotechnology*, 25, 1165. https://doi.org/10.1038/nbt1340

Choi, K., Riviere, J. E., & Monteiro-Riviere, N. A. (2017). Protein corona modulation of hepatocyte uptake and molecular mechanisms of gold nanoparticle toxicity. *Nanotoxicology*, *11*, 64–75. https://doi.org/10.1080/17435390.2016.1264638

Chou, L. Y. T., & Chan, W. C. W. (2012). Fluorescence-tagged gold nanoparticles for rapidly characterizing the size-dependent biodistribution in tumor models. *Advanced Healthcare Materials*, *1*, 714–721. https://doi.org/10.1002/adhm.201200084

Chou, L. Y. T., Zagorovsky, K., & Chan, W. C. W. (2014). DNA assembly of nanoparticle superstructures for controlled biological delivery and elimination. *Nature Nanotechnology*, *9*, 148–155. https://doi.org/10.1038/nnano.2013.309

Conner, S. D., & Schmid, S. L. (2003). Regulated portals of entry into the cell. *Nature*, *422*, 37–44.

Cui, M., Liu, R., Deng, Z., Ge, G., Liu, Y., & Xie, L. (2014). Quantitative study of protein coronas on gold nanoparticles with different surface modifications. *Nano Research*, *7*, 345–352.

Dai, Q., Walkey, C. D., & Chan, W. C. W. (2014). Polyethylene glycol backfilling mitigates the negative impact of the protein corona on nanoparticle cell targeting. *Angewandte Chemie*, *53*, 5093–5096.

Dam, D. H., Culver, K. S., Kandela, I., Lee, R. C., Chandra, K., Lee, H., … Odom, T. W. (2015). Biodistribution and in vivo toxicity of aptamer-loaded gold nanostars. *Nanomedicine: Nanotechnology, Biology and Medicine*, *11*, 671–679.

Danquah, M. K., Zhang, X. A., & Mahato, R. I. (2011). Extravasation of polymeric nanomedicines across tumor vasculature. *Advanced Drug Delivery Reviews*, *63*, 623–639. https://doi.org/10.1016/j.addr.2010.11.005

Davidson, A. M., Brust, M., Cooper, D. L., & Volk, M. (2017). Sensitive analysis of protein adsorption to colloidal gold by differential centrifugal sedimentation. *Analytical Chemistry*, *89*, 6807–6814. https://doi.org/10.1021/acs.analchem.7b01229

Davis, M. E., Chen, Z., & Shin, D. M. (2008). Nanoparticle therapeutics: An emerging treatment modality for cancer. *Nature Reviews Drug Discovery*, *7*, 771–782.

Debbage, P. (2009). Targeted drugs and nanomedicine: Present and future. *Current Pharmaceutical Design*, *15*, 153–172.

Decuzzi, P., & Ferrari, M. (2007). The role of specific and non-specific interactions in receptor-mediated endocytosis of nanoparticles. *Biomaterials*, *28*, 2915–2922.

Decuzzi, P., & Ferrari, M. (2008). The receptor-mediated endocytosis of nonspherical particles. *Biophysical Journal*, *94*, 3790–3797.

Decuzzi, P., Pasqualini, R., Arap, W., & Ferrari, M. (2008). Intravascular delivery of particulate systems: Does geometry really matter? *Pharmaceutical Research*, *26*, 235. https://doi.org/10.1007/s11095-008-9697-x

del Pino, P., Yang, F., Pelaz, B., Zhang, Q., Kantner, K., Hartmann, R., … & Soenen, S. J. (2016). Basic physicochemical properties of polyethylene glycol coated gold nanoparticles that determine their interaction with cells. *Angewandte Chemie International Edition*, *55*, 5483–5487. https://doi.org/10.1002/anie.201511733

Deng, Z. J., Liang, M., Monteiro, M. J., Toth, I., & Minchin, R. F. (2011). Nanoparticle-induced unfolding of fibrinogen promotes mac-1 receptor activation and inflammation. *Nature Nanotechnology*, *6*, 39–44.

Deng, Z. J., Liang, M., Toth, I., Monteiro, M., & Minchin, R. F. (2012a). Plasma protein binding of positively and negatively charged polymer-coated gold nanoparticles elicits different biological responses. *Nanotoxicology*, *7*, 314–322. https://doi.org/10.3109/17435390.2012.655342

Deng, Z. J., Liang, M., Toth, I., Monteiro, M. J., & Minchin, R. F. (2012b). Molecular interaction of poly(acrylic acid) gold nanoparticles with human fibrinogen. *ACS Nano*, *6*, 8962–8969. https://doi.org/10.1021/nn3029953

Deng, Z. J., Mortimer, G., Schiller, T., Musumeci, A., Martin, D., & Minchin, R. F. (2009). Differential plasma protein binding to metal oxide nanoparticles. *Nanotechnology*, *20*, 455101.

Di Carlo, D., Irimia, D., Tompkins, R. G., & Toner, M. (2007). Continuous inertial focusing, ordering, and separation of particles in microchannels. *Proceedings of the National Academy of Sciences of the United States of America*, *104*, 18892–18897. https://doi.org/10.1073/pnas.0704958104

Dinish, U. S., Balasundaram, G., Chang, Y., & Olivo, M. (2015). Actively targeted in vivo multiplex detection of intrinsic Cancer biomarkers using biocompatible SERS Nanotags. *Scientific Reports*, *4*, 4075–4075.

Dixit, V., Den Bossche, J. V., Sherman, D. M., Thompson, D. H., & Andres, R. P. (2006). Synthesis and grafting of Thioctic acid−PEG−folate conjugates onto au nanoparticles for selective targeting of folate receptor-positive tumor cells. *Bioconjugate Chemistry*, *17*, 603–609.

Dobrovolskaia, M. A., & McNeil, S. E. (2007). Immunological properties of engineered nanomaterials. *Nature Nanotechnology*, *2*, 469. https://doi.org/10.1038/nnano.2007.223

Dobrovolskaia, M. A., Patri, A. K., Zheng, J., Clogston, J. D., Ayub, N., Aggarwal, P., … McNeil, S. E. (2009). Interaction of colloidal gold nanoparticles with human blood: Effects on particle size and analysis of plasma protein binding profiles. *Nanomedicine: Nanotechnology, Biology and Medicine*, *5*, 106–117. https://doi.org/10.1016/j.nano.2008.08.001

Dominguez-Medina, S., Kisley, L., Tauzin, L. J., Hoggard, A., Shuang, B., DS Indrasekara, A. S., … Zubarev, E. R. (2016). Adsorption and unfolding of a single protein triggers nanoparticle aggregation. *ACS Nano*, *10*, 2103–2112.

Dorsey, J. F., Sun, L., Joh, D. Y., Witztum, A., Kao, G. D., Alonsobasanta, M., … Tsourkas, A. (2013). Gold nanoparticles in radiation research: Potential applications for imaging and radiosensitization. *Translational Cancer Research*, *2*, 280–291. https://doi.org/10.3978/j.issn.2218-676X.2013.08.09

Doshi, N., & Mitragotri, S. (2010). Macrophages recognize size and shape of their targets. *PLoS One*, *5*, e10051.

Doshi, N., Prabhakarpandian, B., Rea-Ramsey, A., Pant, K., Sundaram, S., & Mitragotri, S. (2010). Flow and adhesion of drug carriers in blood vessels depend on their shape: A study using model synthetic microvascular networks. *Journal of Controlled Release*, *146*, 196–200.

Du, B., Jiang, X., Das, A., Zhou, Q., Yu, M., Jin, R., & Zheng, J. (2017). Glomerular barrier behaves as an atomically precise bandpass filter in a sub-nanometre regime. *Nature Nanotechnology*, *12*, 1096. https://doi.org/10.1038/nnano.2017.170

Elbakry, A., Wurster, E. C., Zaky, A., Liebl, R., Schindler, E., Bauer-Kreisel, P., … Breunig, M. (2012). Layer-by-layer coated gold nanoparticles: Size-dependent delivery of DNA into cells. *Small*, *8*, 3847–3856. https://doi.org/10.1002/smll.201201112

Elsabahy, M., & Wooley, K. L. (2013). Cytokines as biomarkers of nanoparticle immunotoxicity. *Chemical Society Reviews*, *42*, 5552–5576. https://doi.org/10.1039/C3CS60064E

Farokhzad, O. C., & Langer, R. (2009). Impact of nanotechnology on drug delivery. *ACS Nano*, *3*, 16–20.

Feng, G., & Liu, B. (2018). Aggregation-induced emission (AIE) dots: Emerging theranostic nanolights. *Accounts of Chemical Research*, *51*, 1404–1414. https://doi.org/10.1021/acs.accounts.8b00060

Ferro-Flores, G., E Ocampo-García, B., L Santos-Cuevas, C., de Maria Ramirez, F., P Azorin-Vega, E., & Meléndez-Alafort, L. (2015). Theranostic radiopharmaceuticals based on gold nanoparticles labeled with ^{177}Lu and conjugated to peptides. *Current Radiopharmaceuticals*, *8*, 150–159. https://doi.org/10.2174/1874471008666150313115423

Frellsen, A. F., Hansen, A. E., Jølck, R. I., Kempen, P., Severin, G. W., Rasmussen, P. H., … Andresen, T. L. (2016). Mouse positron emission tomography study of the biodistribution of gold nanoparticles with different surface coatings using embedded Copper-64. *ACS Nano*, *10*, 9887–9898. https://doi.org/10.1021/acsnano.6b03144

Friedman, A., Letai, A., Fisher, D. E., & Flaherty, K. T. (2015). Precision medicine for cancer with next-generation functional diagnostics. *Nature Reviews Cancer*, *15*, 747–756.

Gagner, J. E., Lopez, M. D., Dordick, J. S., & Siegel, R. W. (2011). Effect of gold nanoparticle morphology on adsorbed protein structure and function. *Biomaterials*, *32*, 7241–7252. https://doi.org/10.1016/j.biomaterials.2011.05.091

Gao, H., Shi, W., & Freund, L. B. (2005). Mechanics of receptor-mediated endocytosis. *Proceedings of the National Academy of Sciences of the United States of America*, *102*, 9469–9474. https://doi.org/10.1073/pnas.0503879102

Gao, L., Liu, M., Ma, G., Wang, Y., Zhao, L., Yuan, Q., … Gao, X. (2015). Peptide-conjugated gold nanoprobe: Intrinsic nanozyme-linked immunsorbant assay of integrin expression level on cell membrane. *ACS Nano*, *9*, 10979–10990.

Gao, W., Hu, C. M., Fang, R. H., Luk, B. T., Su, J., & Zhang, L. (2013). Surface functionalization of gold nanoparticles with red blood cell membranes. *Advanced Materials*, *25*, 3549–3553.

Gao, X., Qi, Y., Liu, Z., Ke, M., Zhou, X., Li, S., … Li, C. (2017). Guiding brain-tumor surgery via blood–brain-barrier-permeable gold nanoprobes with acid-triggered MRI/SERRS signals. *Advanced Materials*, *29*, 1603917. https://doi.org/10.1002/adma.201603917

Goy-López, S., Juárez, J., Alatorre-Meda, M., Casals, E., Puntes, V. F., Taboada, P., & Mosquera, V. (2012). Physicochemical characteristics of protein–NP bioconjugates: The role of particle curvature and solution conditions on human serum albumin conformation and Fibrillogenesis inhibition. *Langmuir*, *28*, 9113–9126. https://doi.org/10.1021/la300402w

Gu, L., Fang, R. H., Sailor, M. J., & Park, J.-H. (2012). In vivo clearance and toxicity of monodisperse Iron oxide nanocrystals. *ACS Nano*, *6*, 4947–4954. https://doi.org/10.1021/nn300456z

Gunawan, C., Lim, M., Marquis, C. P., & Amal, R. (2014). Nanoparticle-protein corona complexes govern the biological fates and functions of nanoparticles. *Journal of Materials Chemistry B*, *2*, 2060–2083. https://doi.org/10.1039/C3TB21526A

Guo, J., O'Driscoll, C. M., Holmes, J. D., & Rahme, K. (2016). Bioconjugated gold nanoparticles enhance cellular uptake: A proof of concept study for siRNA delivery in prostate cancer cells. *International Journal of Pharmaceutics*, *509*, 16–27. https://doi.org/10.1016/j.ijpharm.2016.05.027

Harrison, E., Nicol, J. R., Maciasmontero, M., Burke, G. A., Coulter, J. A., Meenan, B. J., & Dixon, D. (2016). A comparison of gold nanoparticle surface co-functionalization approaches using polyethylene glycol (PEG) and the effect on stability, non-specific protein adsorption and internalization. *Materials Science and Engineering: C*, *62*, 710–718.

Hauck, T. S., Ghazani, A. A., & Chan, W. C. W. (2008). Assessing the effect of surface chemistry on gold Nanorod uptake, toxicity, and gene expression in mammalian cells. *Small*, *4*, 153–159.

He, J., Unser, S., Bruzas, I., Cary, R., Shi, Z., Mehra, R., … Sagle, L. (2018). The facile removal of CTAB from the surface of gold nanorods. *Colloids and Surfaces B: Biointerfaces*, *163*, 140–145. https://doi.org/10.1016/j.colsurfb.2017.12.019

Hillaireau, H., & Couvreur, P. (2009). Nanocarriers' entry into the cell: Relevance to drug delivery. *Cellular and Molecular Life Sciences*, *66*, 2873–2896.

Hong, R., Han, G., Fernández, J. M., Kim, B. J., Forbes, N. S., & Rotello, V. M. (2006). Glutathione-mediated delivery and release using monolayer protected nanoparticle carriers. *Journal of the American Chemical Society*, *128*, 1078–1079. https://doi.org/10.1021/ja056726i

Hu, R., Yong, K. T., Roy, I., Ding, H., He, S., & Prasad, P. N. (2009). Metallic nanostructures as localized Plasmon resonance enhanced scattering probes for multiplex dark-field targeted imaging of Cancer cells. *The Journal of Physical Chemistry C*, *113*, 2676–2684. https://doi.org/10.1021/jp8076672

Huang, K., Ma, H., Liu, J., Huo, S., Kumar, A., Wei, T., … He, S. (2012). Size-dependent localization and penetration of ultrasmall gold nanoparticles in cancer cells, multicellular spheroids, and tumors in vivo. *ACS Nano*, *6*, 4483–4493. https://doi.org/10.1021/nn301282m

Huang, X., Peng, X., Wang, Y., Wang, Y., Shin, D. M., El-Sayed, M. A., & Nie, S. (2010). A reexamination of active and passive tumor targeting by using rod-shaped gold nanocrystals and covalently conjugated peptide ligands. *ACS Nano*, *4*, 5887–5896. https://doi.org/10.1021/nn102055s

Huang, X., Zhang, F., Zhu, L., Choi, K. Y., Guo, N., Guo, J., … Choi, H. S. (2013). Effect of injection routes on the biodistribution, clearance, and tumor uptake of carbon dots. *ACS Nano*, *7*, 5684–5693. https://doi.org/10.1021/nn401911k

Huang, Y., Sefah, K., Bamrungsap, S., Chang, H., & Tan, W. (2008). Selective photothermal therapy for mixed cancer cells using aptamer-conjugated nanorods. *Langmuir*, *24*, 11860–11865.

Hubbell, J. A., & Chilkoti, A. (2012). Nanomaterials for drug delivery. *Science*, *337*, 303–305. https://doi.org/10.1126/science.1219657

Hühn, D., Kantner, K., Geidel, C., Brandholt, S., De Cock, I., Soenen, S. J., … Nienhaus, G. U. (2013). Polymer-coated nanoparticles interacting with proteins and cells: Focusing on the sign of the net charge. *ACS Nano*, *7*, 3253–3263. https://doi.org/10.1021/nn3059295

Iyer, A. K., Khaled, G., Fang, J., & Maeda, H. (2006). Exploiting the enhanced permeability and retention effect for tumor targeting. *Drug Discovery Today*, *11*, 812–818.

Jain, R. K. (2013). Normalizing tumor microenvironment to treat Cancer: Bench to bedside to biomarkers. *Journal of Clinical Oncology*, *31*, 2205–2218. https://doi.org/10.1200/JCO.2012.46.3653

Jain, R. K., & Stylianopoulos, T. (2010). Delivering nanomedicine to solid tumors. *Nature Reviews. Clinical Oncology*, *7*, 653. https://doi.org/10.1038/nrclinonc.2010.139

Jensen, S. A., Day, E. S., Ko, C. H., Hurley, L. A., Luciano, J. P., Kouri, F. M., … Daniel, W. L. (2013). Spherical nucleic acid nanoparticle conjugates as an RNAi-based therapy for glioblastoma. *Science Translational Medicine*, *5*, 209ra152. https://doi.org/10.1126/scitranslmed.3006839

Jiang, S., & Cao, Z. (2010). Ultralow-fouling, functionalizable, and hydrolyzable Zwitterionic materials and their derivatives for biological applications. *Advanced Materials*, *22*, 920–932.

Jiang, W., Kim, B. Y. S., Rutka, J. T., & Chan, W. C. W. (2008). Nanoparticle-mediated cellular response is size-dependent. *Nature Nanotechnology*, *3*, 145–150.

Jiang, Y., Huo, S., Mizuhara, T., Das, R., Lee, Y. W., Hou, S., … Rotello, V. M. (2015). The interplay of size and surface functionality on the cellular uptake of Sub-10 nm gold nanoparticles. *ACS Nano*, *9*, 9986–9993. https://doi.org/10.1021/acsnano.5b03521

Johnston, B. D., Kreyling, W. G., Pfeiffer, C., Schäffler, M., Sarioglu, H., Ristig, S., … Semmler-Behnke, M. (2017). Colloidal stability and surface chemistry are key factors for the composition of the protein corona of inorganic gold nanoparticles. *Advanced Functional Materials*, *27*, 1701956. https://doi.org/10.1002/adfm.201701956

Kairdolf, B. A., Mancini, M. C., Smith, A. M., & Nie, S. (2008). Minimizing nonspecific cellular binding of quantum dots with hydroxyl-Derivatized surface coatings. *Analytical Chemistry*, *80*, 3029–3034. https://doi.org/10.1021/ac800068q

Kairdolf, B. A., Qian, X., & Nie, S. (2017). Bioconjugated nanoparticles for biosensing, in vivo imaging, and medical diagnostics. *Analytical Chemistry*, *89*, 1015–1031. https://doi.org/10.1021/acs.analchem.6b04873

Kalele, S., Gosavi, S. W., Urban, J., & Kulkarni, S. K. (2006). Nanoshell particles : Synthesis, properties and applications. *Current Science*, *91*, 1038–1052.

Kane, R. S. (2003). Deschatelets, Pascal & Whitesides, G. M. Kosmotropes form the basis of protein-resistant surfaces. *Langmuir*, *19*, 2388–2391.

Karmali, P. P., & Simberg, D. (2011). Interactions of nanoparticles with plasma proteins: Implication on clearance and toxicity of drug delivery systems. *Expert Opinion on Drug Delivery*, *8*, 343–357.

Kato, Y., Ozawa, S., Miyamoto, C., Maehata, Y., Suzuki, A., Maeda, T., & Baba, Y. (2013). Acidic extracellular microenvironment and cancer. *Cancer Cell International*, *13*, 89–89.

Kaur, K., & Forrest, J. A. (2012). Influence of particle size on the binding activity of proteins adsorbed onto gold nanoparticles. *Langmuir*, *28*, 2736–2744. https://doi.org/10.1021/la203528u

Kersey, F. R., Merkel, T. J., Perry, J. L., Napier, M. E., & Desimone, J. M. (2012). Effect of aspect ratio and deformability on nanoparticle extravasation through nanopores. *Langmuir*, *28*, 8773–8781.

Kessenbrock, K., Plaks, V., & Werb, Z. (2010). Matrix metalloproteinases: Regulators of the tumor microenvironment. *Cell*, *141*, 52–67.

Khlebtsov, N., & Dykman, L. (2011). Biodistribution and toxicity of engineered gold nanoparticles: A review of in vitro and in vivo studies. *Chemical Society Reviews*, *40*, 1647–1671. https://doi.org/10.1039/C0CS00018C

Kim, D., Jeong, Y. Y., & Jon, S. (2010). A drug-loaded aptamer-gold nanoparticle bioconjugate for combined CT imaging and therapy of prostate cancer. *ACS Nano*, *4*, 3689–3696.

Kim, S. M., Faix, P. H., & Schnitzer, J. E. (2017). Overcoming key biological barriers to cancer drug delivery and efficacy. *Journal of Controlled Release*, *267*, 15–30. https://doi.org/10.1016/j.jconrel.2017.09.016

Kinnear, C., Moore, T. L., Rodriguez-Lorenzo, L., Rothen-Rutishauser, B., & Petri-Fink, A. (2017). Form follows function: Nanoparticle shape and its implications for nanomedicine. *Chemical Reviews*, *117*, 11476–11521. https://doi.org/10.1021/acs.chemrev.7b00194

Kolosnjaj-Tabi, J., Javed, Y., Lartigue, L., Volatron, J., Elgrabli, D., Marangon, I., … Pellegrino, T. (2015). The one year fate of Iron oxide coated gold nanoparticles in mice. *ACS Nano*, *9*, 7925–7939. https://doi.org/10.1021/acsnano.5b00042

Kumar, P. S., Pastorizasantos, I., Rodriguezgonzalez, B., De Abajo, F. J. G., & Lizmarzan, L. M. (2008). High-yield synthesis and optical response of gold nanostars. *Nanotechnology*, *19*, 015606.

Kumar, R., Roy, I., Ohulchanskky, T. Y., Vathy, L. A., Bergey, E. J., Sajjad, M., & Prasad, P. N. (2010). In vivo biodistribution and clearance studies using multimodal organically modified silica nanoparticles. *ACS Nano*, *4*, 699–708. https://doi.org/10.1021/nn901146y

Lacerda, S. H. D. P., Park, J. J., Meuse, C., Pristinski, D., Becker, M. L., Karim, A., & Douglas, J. F. (2010). Interaction of gold nanoparticles with common human blood proteins. *ACS Nano*, *4*, 365–379. https://doi.org/10.1021/nn9011187

Lammers, T., Hennink, W. E., & Storm, G. (2008). Tumour-targeted nanomedicines: Principles and practice. *British Journal of Cancer*, *99*, 392–397.

Lane, L. A., Qian, X., & Nie, S. (2015). SERS nanoparticles in medicine: From label-free detection to spectroscopic tagging. *Chemical Reviews*, *115*, 10489–10529.

Lane, L. A., Qian, X., Smith, A. M., & Nie, S. (2015). Physical chemistry of nanomedicine: Understanding the complex behaviors of nanoparticles in vivo. *Annual Review of Physical Chemistry*, *66*, 521–547.

Langille, M. R., Personick, M. L., Zhang, J., & Mirkin, C. A. (2012). Defining rules for the shape evolution of gold nanoparticles. *Journal of the American Chemical Society*, *134*, 14542–14554.

Laughlin, R. G. (1991). Fundamentals of the zwitterionic hydrophilic group. *Langmuir*, *7*, 842–847. https://doi.org/10.1021/la00053a006

Leckband, D. E. (2000). Measuring the forces that control protein interactions. *Annual Review of Biophysics and Biomolecular Structure*, *29*, 1–26.

Leckband, D. E., & Israelachvili, J. N. (2001). Intermolecular forces in biology. *Quarterly Reviews of Biophysics*, *34*, 105–267.

Lee, H., & Larson, R. G. (2016). Adsorption of plasma proteins onto PEGylated lipid bilayers: The effect of PEG size and grafting density. *Biomacromolecules*, *17*, 1757–1765. https://doi.org/10.1021/acs.biomac.6b00146

Lee, S. B., Yoon, G., Lee, S. W., Jeong, S. Y., Ahn, B. C., Lim, D. K., … Jeon, Y. H. (2016). Combined positron emission tomography and Cerenkov luminescence imaging of sentinel lymph nodes using PEGylated radionuclide-embedded gold nanoparticles. *Small*, *12*, 4894–4901. https://doi.org/10.1002/smll.201601721

Li, H. J., Du, J. Z., Du, X. J., Xu, C. F., Sun, C. Y., Wang, H. X., … Wang, J. (2016a). Stimuli-responsive clustered nanoparticles for improved tumor penetration and therapeutic efficacy. *Proceedings of the National Academy of Sciences of the United States of America*, *113*, 4164–4169. https://doi.org/10.1073/pnas.1522080113

Li, N., Zhao, P., & Astruc, D. (2014). Anisotropic gold nanoparticles: Synthesis, properties, applications, and toxicity. *Angewandte Chemie*, *53*, 1756–1789.

Li, S.-D., & Huang, L. (2008). Pharmacokinetics and biodistribution of nanoparticles. *Molecular Pharmaceutics*, *5*, 496–504. https://doi.org/10.1021/mp800049w

Li, W., & Chen, X. (2015). Gold nanoparticles for photoacoustic imaging. *Nanomedicine: Nanotechnology, Biology and Medicine*, *10*, 299–320.

Li, Y., & Monteiro-Riviere, N. A. (2016). Mechanisms of cell uptake, inflammatory potential and protein corona effects with gold nanoparticles. *Nanomedicine*, *11*, 3185–3203. https://doi.org/10.2217/nnm-2016-0303

Li, Z., Tang, S., Wang, B., Li, Y., Huang, H., Wang, H., … Yu, X. F. (2016b). Metabolizable small gold nanorods: Size-dependent cytotoxicity. *Cell Uptake and in vivo Biodistribution. ACS Biomaterials Science & Engineering*, *2*, 789–797. https://doi.org/10.1021/acsbiomaterials.5b00538

Liang, M., Lin, I. C., Whittaker, M. R., Minchin, R. F., Monteiro, M. J., & Toth, I. (2010). Cellular uptake of densely packed polymer coatings on gold nanoparticles. *ACS Nano*, *4*, 403–413.

Lin, Z., Monteiroriviere, N. A., & Riviere, J. E. (2015). Pharmacokinetics of metallic nanoparticles. *WIREs Nanomedicine and Nanobiotechnology*, *7*, 189–217.

Lipka, J., Semmler-Behnke, M., Sperling, R. A., Wenk, A., Takenaka, S., Schleh, C., … Kreyling, W. G. (2010). Biodistribution of PEG-modified gold nanoparticles following intratracheal instillation and intravenous injection. *Biomaterials*, *31*, 6574–6581.

Liu, J., Yu, M., Zhou, C., Yang, S., Ning, X., & Zheng, J. (2013b). Passive tumor targeting of renal-clearable luminescent gold nanoparticles: Long tumor retention and fast normal tissue clearance. *Journal of the American Chemical Society*, *135*, 4978–4981. https://doi.org/10.1021/ja401612x

Liu, J., Yu, M., Ning, X., Zhou, C., Yang, S., & Zheng, J. (2013c). PEGylation and Zwitterionization: Pros and cons in the renal clearance and tumor targeting of near-IR-emitting gold nanoparticles. *Angewandte Chemie International Edition*, *52*, 12572–12576. https://doi.org/10.1002/anie.201304465

Liu, J., Duchesne, P. N., Yu, M., Jiang, X., Ning, X., Vinluan III, R. D., … Zheng, J. (2016). Luminescent gold nanoparticles with size-independent emission. *Angewandte Chemie*, *55*, 8894–8898.

Liu, X., Huang, N., Li, H., Jin, Q., & Ji, J. (2013). Surface and size effects on cell interaction of gold nanoparticles with both phagocytic and nonphagocytic cells. *Langmuir*, *29*, 9138–9148.

Liu, X., Li, H., Chen, Y., Jin, Q., Ren, K., & Ji, J. (2014). Mixed-charge nanoparticles for long circulation, low reticuloendothelial system clearance, and high tumor accumulation. *Advanced Healthcare Materials*, *3*, 1439–1447. https://doi.org/10.1002/adhm.201300617

Liu, Y., Wang, Z., Liu, Y., Zhu, G., Jacobson, O., Fu, X., … Fan, W. (2017). Suppressing nanoparticle-mononuclear phagocyte system interactions of two-dimensional gold Nanorings for improved tumor accumulation and photothermal ablation of tumors. *ACS Nano*, *11*, 10539–10548. https://doi.org/10.1021/acsnano.7b05908

Longmire, M., Choyke, P. L., & Kobayashi, H. (2008). Clearance properties of nano-sized particles and molecules as imaging agents: Considerations and caveats. *Nanomedicine*, *3*, 703–717. https://doi.org/10.2217/17435889.3.5.703

Love, J. C., Estroff, L. A., Kriebel, J. K., Nuzzo, R. G., & Whitesides, G. M. (2005). Self-assembled monolayers of thiolates on metals as a form of nanotechnology. *Chemical Reviews*, *105*, 1103–1169.

Lu, W., Xiong, C., Zhang, R., Shi, L., Huang, M., Zhang, G., … Li, C. (2012). Receptor-mediated transcytosis: A mechanism for active extravascular transport of nanoparticles in solid tumors. *Journal of Controlled Release*, *161*, 959–966. https://doi.org/10.1016/j.jconrel.2012.05.014

Lundqvist, M., Stigler, J., Elia, G., Lynch, I., Cedervall, T., & Dawson, K. A. (2008). Nanoparticle size and surface properties determine the protein corona with possible implications for biological impacts. *Proceedings of the National Academy of Sciences of the United States of America*, *105*, 14265–14270. https://doi.org/10.1073/pnas.0805135105

Lynch, I., & Dawson, K. A. (2008). Protein-nanoparticle interactions. *Nano Today*, *3*, 40–47. https://doi.org/10.1016/S1748-0132(08)70014-8

Ma, Z., Bai, J., Wang, Y., & Jiang, X. (2014). Impact of shape and pore size of mesoporous silica nanoparticles on serum protein adsorption and RBCs hemolysis. *ACS Applied Materials & Interfaces*, *6*, 2431–2438. https://doi.org/10.1021/am404860q

Mahmoudi, M., Lynch, I., Ejtehadi, M. R., Monopoli, M. P., Bombelli, F. B., & Laurent, S. (2011). Protein−nanoparticle interactions: Opportunities and challenges. *Chemical Reviews*, *111*, 5610–5637. https://doi.org/10.1021/cr100440g

Mansoori, G. A., Brandenburg, K. S., & Shakerizadeh, A. (2010). A comparative study of two folate-conjugated gold nanoparticles for cancer nanotechnology applications. *Cancers*, *2*, 1911–1928.

Matsumura, Y., & Maeda, H. (1986). A new concept for macromolecular therapeutics in cancer chemotherapy: Mechanism of Tumoritropic accumulation of proteins and the antitumor agent Smancs. *Cancer Research*, *46*, 6387–6392.

McDonald, D. M., Thurston, G., & Baluk, P. (1999). Endothelial gaps as sites for plasma leakage in inflammation. *Microcirculation*, *6*, 7–22. https://doi.org/10.1111/j.1549-8719.1999.tb00084.x

Mehtala, J. G., Zemlyanov, D. Y., Max, J. P., Kadasala, N., Zhao, S., & Wei, A. (2014). Citrate-stabilized gold nanorods. *Langmuir*, *30*, 13727–13730. https://doi.org/10.1021/la5029542

Mei, K.-C., Bai, J., Lorrio, S., Wang, J. T.-W., & Al-Jamal, K. T. (2016). Investigating the effect of tumor vascularization on magnetic targeting in vivo using retrospective design of experiment. *Biomaterials*, *106*, 276–285. https://doi.org/10.1016/j.biomaterials.2016.08.030

Melancon, M. P., Lu, W., Yang, Z., Zhang, R., Cheng, Z., Elliot, A. M., … Li, C. (2008). In vitro and in vivo targeting of hollow gold nanoshells directed at epidermal growth factor receptor for photothermal ablation therapy. *Molecular Cancer Therapeutics*, *7*, 1730–1739.

Melancon, M. P., Zhou, M., Zhang, R., Xiong, C., Allen, P., Wen, X., … Liang, D. (2014). Selective uptake and imaging of aptamer- and antibody-conjugated hollow Nanospheres targeted to epidermal growth factor receptors overexpressed in head and neck Cancer. *ACS Nano*, *8*, 4530–4538. https://doi.org/10.1021/nn406632u

Melby, E. S., Lohse, S. E., Park, J. E., Vartanian, A. M., Putans, R. A., Abbott, H. B., … Pedersen, J. A. (2017). Cascading effects of nanoparticle coatings: Surface functionalization dictates the assemblage of complexed proteins and subsequent interaction with model cell membranes. *ACS Nano*, *11*, 5489–5499. https://doi.org/10.1021/acsnano.7b00231

Meyer, R. A., & Green, J. J. (2016). Shaping the future of nanomedicine: Anisotropy in polymeric nanoparticle design. *WIREs Nanomedicine and Nanobiotechnology*, *8*, 191–207. https://doi.org/10.1002/wnan.1348

Miao, L., & Huang, L. (2015). In C. A. Mirkin, T. J. Meade, S. H. Petrosko, & A. H. Stegh (Eds.), *Nanotechnology-Based Precision Tools for the Detection and Treatment of Cancer* (pp. 193–226). Switzerland: Springer International Publishing.

Miao, L., Newby, J. M., Lin, C. M., Zhang, L., Xu, F., Kim, W. Y., … Huang, L. (2016). The binding site barrier elicited by tumor-associated fibroblasts interferes disposition of nanoparticles in stroma-vessel type tumors. *ACS Nano*, *10*, 9243–9258.

Millstone, J. E., Hurst, S. J., Metraux, G. S., Cutler, J. I., & Mirkin, C. A. (2009). Colloidal gold and silver triangular Nanoprisms. *Small*, *5*, 646–664.

Millstone, J. E., Wei, W., Jones, M. R., Yoo, H., & Mirkin, C. A. (2008). Iodide ions control seed-mediated growth of anisotropic gold nanoparticles. *Nano Letters*, *8*, 2526–2529. https://doi.org/10.1021/nl8016253

Moderypawlowski, C. L., & Gupta, A. S. (2014). Heteromultivalent ligand-decoration for actively targeted nanomedicine. *Biomaterials*, *35*, 2568–2579.

Monopoli, M. P., Aberg, C., Salvati, A., & Dawson, K. A. (2012). Biomolecular coronas provide the biological identity of nanosized materials. *Nature Nanotechnology*, *7*, 779–786.

Monopoli, M. P., Walczyk, D., Campbell, A., Elia, G., Lynch, I., Baldelli Bombelli, F., & Dawson, K. A. (2011). Physical−chemical aspects of protein corona: Relevance to in vitro and in vivo biological impacts of nanoparticles. *Journal of the American Chemical Society*, *133*, 2525–2534. https://doi.org/10.1021/ja107583h

Moon, J. J., Huang, B., & Irvine, D. J. (2012). Engineering nano- and microparticles to tune immunity. *Advanced Materials*, *24*, 3724–3746. https://doi.org/10.1002/adma.201200446

Mosquera, J., Henriksen-Lacey, M., García, I., Martínez-Calvo, M., Rodríguez, J., Mascareñas, J. L., & Liz-Marzán, L. M. (2018). Cellular uptake of gold nanoparticles triggered by host–guest interactions. *Journal of the American Chemical Society*, *140*, 4469–4472. https://doi.org/10.1021/jacs.7b12505

Moyano, D. F., Goldsmith, M., Solfiell, D. J., Landesman-Milo, D., Miranda, O. R., Peer, D., & Rotello, V. M. (2012). Nanoparticle hydrophobicity dictates immune response. *Journal of the American Chemical Society*, *134*, 3965–3967.

Murphy, C. J., Thompson, L. B., Alkilany, A. M., Sisco, P. N., Boulos, S. P., Sivapalan, S. T., … Huang, J. (2010). The many faces of gold Nanorods. *Journal of Physical Chemistry Letters*, *1*, 2867–2875.

Nakagawa, T., Gonda, K., Kamei, T., Cong, L., Hamada, Y., Kitamura, N., … Nakano, Y. (2016). X-ray computed tomography imaging of a tumor with high sensitivity using gold nanoparticles conjugated to a cancer-specific antibody via polyethylene glycol chains on their surface. *Science and Technology of Advanced Materials*, *17*, 387–397. https://doi.org/10.1080/14686996.2016.1194167

Nath, N., Hyun, J., Ma, H., & Chilkoti, A. (2004). Surface engineering strategies for control of protein and cell interactions. *Surface Science*, *570*, 98–110. https://doi.org/10.1016/j.susc.2004.06.182

Nel, A. E., Mädler, L., Velegol, D., Xia, T., Hoek, E. M., Somasundaran, P., … Thompson, M. (2009). Understanding biophysicochemical interactions at the nano–bio interface. *Nature Materials*, *8*, 543. https://doi.org/10.1038/nmat2442

Nie, S. (2010). Understanding and overcoming major barriers in cancer nanomedicine. *Nanomedicine: Nanotechnology, Biology and Medicine*, *5*, 523–528.

Ning, X., Peng, C., Li, E. S., Xu, J., Vinluan III, R. D., Yu, M., & Zheng, J. (2017). Physiological stability and renal clearance of ultrasmall zwitterionic gold nanoparticles: Ligand length matters. *APL Materials*, *5*, 053406.

Niu, W., Chua, Y. A. A., Zhang, W., Huang, H., & Lu, X. (2015). Highly symmetric gold Nanostars: Crystallographic control and surface-enhanced Raman scattering property. *Journal of the American Chemical Society*, *137*, 10460–10463.

Nowinski, A. K., White, A. D., Keefe, A. J., & Jiang, S. (2014). Biologically inspired stealth peptide-capped gold nanoparticles. *Langmuir*, *30*, 1864–1870. https://doi.org/10.1021/la404980g

Obrien, M. N., Jones, M. R., Brown, K. A., & Mirkin, C. A. (2014). Universal Noble metal nanoparticle seeds realized through iterative reductive growth and oxidative dissolution reactions. *Journal of the American Chemical Society*, *136*, 7603–7606.

Oh, N., & Park, J. (2014b). Endocytosis and exocytosis of nanoparticles in mammalian cells. *International Journal of Nanomedicine*, *9*, 51–63.

Oh, N., & Park, J.-H. (2014a). Surface chemistry of gold nanoparticles mediates their exocytosis in macrophages. *ACS Nano*, *8*, 6232–6241. https://doi.org/10.1021/nn501668a

Ojeajimenez, I., Garciafernandez, L., Lorenzo, J., & Puntes, V. (2012). Facile preparation of cationic gold nanoparticle-bioconjugates for cell penetration and nuclear targeting. *ACS Nano*, *6*, 7692–7702.

Oldenborg, P. A., Zheleznyak, A., Fang, Y. F., Lagenaur, C. F., Gresham, H. D., & Lindberg, F. P. (2000). Role of CD47 as a marker of self on red blood cells. *Science*, *288*, 2051–2054.

Otsuka, H., Nagasaki, Y., & Kataoka, K. (2003). PEGylated nanoparticles for biological and pharmaceutical applications. *Advanced Drug Delivery Reviews*, *55*, 403–419.

Owens, D. E., & Peppas, N. A. (2006). Opsonization, biodistribution, and pharmacokinetics of polymeric nanoparticles. *International Journal of Pharmaceutics*, *307*, 93–102.

Peer, D., Karp, J. M., Hong, S., Farokhzad, O. C., Margalit, R., & Langer, R. (2007). Nanocarriers as an emerging platform for cancer therapy. *Nature Nanotechnology*, *2*, 751. https://doi.org/10.1038/nnano.2007.387

Perrault, S. D., Walkey, C., Jennings, T., Fischer, H. C., & Chan, W. C. W. (2009). Mediating tumor targeting efficiency of nanoparticles through design. *Nano Letters*, *9*, 1909–1915. https://doi.org/10.1021/nl900031y

Petros, R. A., & Desimone, J. M. (2010). Strategies in the design of nanoparticles for therapeutic applications. *Nature Reviews Drug Discovery*, *9*, 615–627.

Pham, T., & Jackson, J. B. (2002). Halas, J, N. & lee, T. R. Preparation and characterization of gold nanoshells coated with self-assembled monolayers. *Langmuir*, *18*, 4915–4920.

Pirollo, K. F., & Chang, E. H. (2008). Does a targeting ligand influence nanoparticle tumor localization or uptake. *Trends in Biotechnology*, 26, 552–558.

Pissuwan, D., Valenzuela, S. M., Killingsworth, M. C., Xu, X., & Cortie, M. B. (2007). Targeted destruction of murine macrophage cells with bioconjugated gold nanorods. *Journal of Nanoparticle Research*, 9, 1109–1124.

Popovtzer, R., Agrawal, A., Kotov, N. A., Popovtzer, A., Balter, J., Carey, T. E., & Kopelman, R. (2008). Targeted gold nanoparticles enable molecular CT imaging of cancer. *Nano Letters*, 8, 4593–4596.

Prabhakar, U., Maeda, H., Jain, R. K., Sevick-Muraca, E. M., Zamboni, W., Farokhzad, O. C., … Blakey, D. C. (2013). Challenges and key considerations of the enhanced permeability and retention effect for nanomedicine drug delivery in oncology. *Cancer Research*, 73, 2412–2417.

Qian, X., Ansari, D., & Nie, S. (2007). In vivo tumor targeting and spectroscopic detection with surface-enhanced Raman nanoparticle tags. *Nature Biotechnology*, 26, 83–90.

Rahman, M., Laurent, S., Tawil, N., Yahia, L. H., & Mahmoudi, M. (2013). In M. Rahman, et al. (Eds.), *Protein-nanoparticle interactions: The bio-nano interface* (pp. 21–44). Berlin, Germany: Springer.

Rejiya, C. S., Kumar, J., Raji, V., Vibin, M., & Abraham, A. (2012). Laser immunotherapy with gold nanorods causes selective killing of tumour cells. *Pharmacological Research*, 65, 261–269. https://doi.org/10.1016/j.phrs.2011.10.005

Richards, D. A., Maruani, A., & Chudasama, V. (2017). Antibody fragments as nanoparticle targeting ligands: A step in the right direction. *Chemical Science*, 8, 63–77.

Romberg, B., Oussoren, C., Snel, C. J., Carstens, M. G., Hennink, W. E., & Storm, G. (2007). Pharmacokinetics of poly(hydroxyethyl-l-asparagine)-coated liposomes is superior over that of PEG-coated liposomes at low lipid dose and upon repeated administration. *Biochimica et Biophysica Acta (BBA) - Biomembranes*, 1768, 737–743. https://doi.org/10.1016/j.bbamem.2006.12.005

Ruan, Q., Shao, L., Shu, Y., Wang, J., & Wu, H. (2014). Growth of monodisperse gold nanospheres with diameters from 20 nm to 220 nm and their Core/satellite nanostructures. *Advanced Optical Materials*, 2, 65–73. https://doi.org/10.1002/adom.201300359

Ruan, S., Hu, C., Tang, X., Cun, X., Xiao, W., Shi, K., … Gao, H. (2016). Increased gold nanoparticle retention in brain tumors by in situ enzyme-induced aggregation. *ACS Nano*, 10, 10086–10098. https://doi.org/10.1021/acsnano.6b05070

Ruggiero, A., Villa, C. H., Bander, E., Rey, D. A., Bergkvist, M., Batt, C. A., … McDevitt, M. R. (2010). Paradoxical glomerular filtration of carbon nanotubes. *Proceedings of the National Academy of Sciences of the United States of America*, 107, 12369–12374. https://doi.org/10.1073/pnas.0913667107

Ruoslahti, E., Bhatia, S. N., & Sailor, M. J. (2010). Targeting of drugs and nanoparticles to tumors. *Journal of Cell Biology*, 188, 759–768.

Sadauskas, E., Danscher, G., Stoltenberg, M., Vogel, U., Larsen, A., & Wallin, H. (2009). Protracted elimination of gold nanoparticles from mouse liver. *Nanomedicine: Nanotechnology, Biology and Medicine*, 5, 162–169. https://doi.org/10.1016/j.nano.2008.11.002

Saga, T., Neumann, R. D., Heya, T., Sato, J., Kinuya, S., Le, N., … Weinstein, J. N. (1995). Targeting cancer micrometastases with monoclonal antibodies : A binding-site barrier. *Proceedings of the National Academy of Sciences of the United States of America*, 92, 8999–9003.

Scarabelli, L., Coronadopuchau, M., Ginercasares, J. J., Langer, J., & Lizmarzan, L. M. (2014). Monodisperse gold Nanotriangles: Size control, large-scale self-assembly, and performance in surface-enhanced Raman scattering. *ACS Nano*, 8, 5833–5842.

Schlenoff, J., & Zwitteration, B. (2014). Coating surfaces with Zwitterionic functionality to reduce nonspecific adsorption. *Langmuir*, 30, 9625–9636.

Schöttler, S., Becker, G., Winzen, S., Steinbach, T., Mohr, K., Landfester, K., … Wurm, F. R. (2016). Protein adsorption is required for stealth effect of poly(ethylene glycol)- and poly(phosphoester)-coated nanocarriers. *Nature Nanotechnology*, 11, 372–377. https://doi.org/10.1038/nnano.2015.330

Schulz, F., Friedrich, W., Hoppe, K., Vossmeyer, T., Weller, H., & Lange, H. (2016). Effective PEGylation of gold nanorods. *Nanoscale*, 8, 7296–7308. https://doi.org/10.1039/C6NR00607H

Sei-Young, L., Mauro, F., & Paolo, D. (2009). Shaping nano−/micro-particles for enhanced vascular interaction in laminar flows. *Nanotechnology*, 20, 495101.

Semmler-Behnke, M., Kreyling, W. G., Lipka, J., Fertsch, S., Wenk, A., Takenaka, S., … Brandau, W. (2008). Biodistribution of 1.4- and 18-nm gold particles in rats. *Small*, 4, 2108–2111. https://doi.org/10.1002/smll.200800922

Shao, Q., & Jiang, S. (2013). Effect of carbon spacer length on Zwitterionic carboxybetaines. *The Journal of Physical Chemistry B*, 117, 1357–1366. https://doi.org/10.1021/jp3094534

Shao, Q., & Jiang, S. (2014). Influence of charged groups on the properties of Zwitterionic moieties: A molecular simulation study. *The Journal of Physical Chemistry B*, 118, 7630–7637. https://doi.org/10.1021/jp5027114

Shao, Q., White, A. D., & Jiang, S. (2014). Difference of carboxybetaine and oligo(ethylene glycol) moieties in altering hydrophobic interactions: A molecular simulation study. *The Journal of Physical Chemistry B*, 118, 189–194. https://doi.org/10.1021/jp410224w

Shilo, M., Reuveni, T., Motiei, M., & Popovtzer, R. (2012). Nanoparticles as computed tomography contrast agents: Current status and future perspectives. *Nanomedicine: Nanotechnology, Biology and Medicine*, 7, 257–269.

Shukla, R., Bansal, V., Chaudhary, M., Basu, A., Bhonde, R. R., & Sastry, M. (2005). Biocompatibility of gold nanoparticles and their endocytotic fate inside the cellular compartment: A microscopic overview. *Langmuir*, 21, 10644–10654.

Skrabalak, S. E., Chen, J., Sun, Y., Lu, X., Au, L., Cobley, C. M., & Xia, Y. (2008). Gold Nanocages: Synthesis, properties, and applications. *Accounts of Chemical Research*, 41, 1587–1595.

Smith, B. R., & Gambhir, S. S. (2017). Nanomaterials for in vivo imaging. *Chemical Reviews*, 117, 901–986. https://doi.org/10.1021/acs.chemrev.6b00073

Stylianopoulos, T., & Jain, R. K. (2015). Design considerations for nanotherapeutics in oncology. *Nanomedicine: Nanotechnology, Biology and Medicine*, 11, 1893–1907. https://doi.org/10.1016/j.nano.2015.07.015

Sun, T., Zhang, Y. S., Pang, B., Hyun, D. C., Yang, M., & Xia, Y. (2014a). Engineered nanoparticles for drug delivery in cancer therapy. *Angewandte Chemie International Edition*, 53, 12320–12364. https://doi.org/10.1002/anie.201403036

Sun, X., Huang, X., Yan, X., Wang, Y., Guo, J., Jacobson, O., … Kiesewetter, D. O. (2014b). Chelator-free 64Cu-integrated gold nanomaterials for positron emission tomography imaging guided photothermal cancer therapy. *ACS Nano*, 8, 8438–8446.

Sun, Y., Feng, W., Yang, P., Huang, C., & Li, F. (2015). The biosafety of lanthanide upconversion nanomaterials. *Chemical Society Reviews*, 44, 1509–1525. https://doi.org/10.1039/C4CS00175C

Sykes, E. A., Chen, J., Zheng, G., & Chan, W. C. W. (2014). Investigating the impact of nanoparticle size on active and passive tumor targeting efficiency. *ACS Nano*, 8, 5696–5706. https://doi.org/10.1021/nn500299p

Talamini, L., Violatto, M. B., Cai, Q., Monopoli, M. P., Kantner, K., Krpetić, Z., … Boselli, L. (2017). Influence of size and shape on the anatomical distribution of endotoxin-free gold nanoparticles. *ACS Nano*, 11, 5519–5529. https://doi.org/10.1021/acsnano.7b00497

Tan, J., Shah, S., Thomas, A., Ouyang, H. D., & Liu, Y. (2013). The influence of size, shape and vessel geometry on nanoparticle distribution. *Microfluidics and Nanofluidics*, 14, 77–87.

Tang, S., Chen, M., & Zheng, N. (2014). Sub-10-nm Pd Nanosheets with renal clearance for efficient near-infrared photothermal cancer therapy. *Small*, 10, 3139–3144. https://doi.org/10.1002/smll.201303631

Tang, S., Peng, C., Xu, J., Du, B., Wang, Q., Vinluan III, R. D., … Zheng, J. (2016). Tailoring renal clearance and tumor targeting of ultrasmall metal nanoparticles with particle density. *Angewandte Chemie*, 55, 16039–16043.

Tarantola, M., Pietuch, A., Schneider, D., Rother, J., Sunnick, E., Rosman, C., … Janshoff, A. (2011). Toxicity of gold-nanoparticles: Synergistic effects of shape and surface functionalization on micromotility of epithelial cells. *Nanotoxicology*, 5, 254–268.

Tay, C. Y., Setyawati, M. I., Xie, J., Parak, W. J., & Leong, D. T. (2014). Back to basics: Exploiting the innate physico-chemical characteristics of nanomaterials for biomedical applications. *Advanced Functional Materials*, 24, 5936–5955. https://doi.org/10.1002/adfm.201401664

Tenzer, S., Docter, D., Kuharev, J., Musyanovych, A., Fetz, V., Hecht, R., … Landfester, K. (2013). Rapid formation of plasma protein corona critically affects nanoparticle pathophysiology. *Nature Nanotechnology*, 8, 772. https://doi.org/10.1038/nnano.2013.181

Thakor, A. S., Luong, R., Paulmurugan, R., Lin, F. I., Kempen, P., Zavaleta, C., … Gambhir, S. S. The fate and toxicity of Raman-active silica-gold nanoparticles in mice. *Science Translational Medicine*, 3, 79ra33–79ra33. https://doi.org/10.1126/scitranslmed.3001963

Tong, X., Wang, Z., Sun, X., Song, J., Jacobson, O., Niu, G., … Chen, X. (2016). Size dependent kinetics of gold nanorods in EPR mediated tumor delivery. *Theranostics*, 6, 2039–2051.

Le Tourneau, C., Delord, J. P., Gonçalves, A., Gavoille, C., Dubot, C., Isambert, N., … Armanet, S. (2015). Molecularly targeted therapy based on tumour molecular profiling versus conventional therapy for advanced cancer (SHIVA): A multicentre, open-label, proof-of-concept, randomised, controlled phase 2 trial. *Lancet Oncology*, 16, 1324–1334.

Toy, R., Hayden, E., Shoup, C., Baskaran, H., & Karathanasis, E. (2011). The effects of particle size, density and shape on margination of nanoparticles in microcirculation. *Nanotechnology*, 22, 115101–115101.

Toy, R., Peiris, P. M., Ghaghada, K. B., & Karathanasis, E. (2014). Shaping cancer nanomedicine: The effect of particle shape on the in vivo journey of nanoparticles. *Nanomedicine*, 9, 121–134. https://doi.org/10.2217/nnm.13.191

Trouiller, A. J., Hebié, S., el Bahhaj, F., Napporn, T. W., & Bertrand, P. (2015). Chemistry for oncotheranostic gold nanoparticles. *European Journal of Medicinal Chemistry*, 99, 92–112. https://doi.org/10.1016/j.ejmech.2015.05.024

Tsai, R. K., Rodriguez, P. L., & Discher, D. E. (2010). Self inhibition of phagocytosis: The affinity of 'marker of self' CD47 for SIRPα dictates potency of inhibition but only at low expression levels. *Blood Cells, Molecules & Diseases*, 45, 67–74.

Tsoi, K. M., MacParland, S. A., Ma, X. Z., Spetzler, V. N., Echeverri, J., Ouyang, B., … Conneely, J. B. (2016). Mechanism of hard-nanomaterial clearance by the liver. *Nature Materials*, 15, 1212–1221.

Ulman, A. (1996). Formation and structure of self-assembled monolayers. *Chemical Reviews*, 96, 1533–1554.

Venkataraman, S., Hedrick, J. L., Ong, Z. Y., Yang, C., Ee, P. L. R., Hammond, P. T., & Yang, Y. Y. (2011). The effects of polymeric nanostructure shape on drug delivery. *Advanced Drug Delivery Reviews*, 63, 1228–1246.

Vilanova, O., Mittag, J. J., Kelly, P. M., Milani, S., Dawson, K. A., Rädler, J. O., & Franzese, G. (2016). Understanding the kinetics of protein–nanoparticle corona formation. *ACS Nano*, 10, 10842–10850.

Vinluan, R. D., III, & Zheng, J. (2015). Serum protein adsorption and excretion pathways of metal nanoparticles. *Nanomedicine*, 10, 2781–2794. https://doi.org/10.2217/nnm.15.97

Vinluan III, R. D., Liu, J., Zhou, C., Yu, M., Yang, S., Kumar, A., … Zheng, J. (2014). Glutathione-coated luminescent gold nanoparticles: A surface ligand for minimizing serum protein adsorption. *ACS Applied Materials & Interfaces*, 6, 11829–11833. https://doi.org/10.1021/am5031374

Walkey, C. D., & Chan, W. C. W. (2012). Understanding and controlling the interaction of nanomaterials with proteins in a physiological environment. *Chemical Society Reviews*, 41, 2780–2799. https://doi.org/10.1039/C1CS15233E

Walkey, C. D., Olsen, J. B., Guo, H., Emili, A., & Chan, W. C. W. (2012). Nanoparticle size and surface chemistry determine serum protein adsorption and macrophage uptake. *Journal of the American Chemical Society*, 134, 2139–2147. https://doi.org/10.1021/ja2084338

Walkey, C. D., Olsen, J. B., Song, F., Liu, R., Guo, H., Olsen, D. W. H., … Chan, W. C. (2014). Protein corona fingerprinting predicts the cellular interaction of gold and silver nanoparticles. *ACS Nano*, 8, 2439–2455. https://doi.org/10.1021/nn406018q

Wang, H., Zheng, L., Peng, C., Shen, M., Shi, X., & Zhang, G. (2013b). Folic acid-modified dendrimer-entrapped gold nanoparticles as nanoprobes for targeted CT imaging of human lung adencarcinoma. *Biomaterials*, 34, 470–480.

Wang, J. Y., Chen, J., Yang, J., Wang, H., Shen, X., Sun, Y. M., … Zhang, X. D. (2016). Effects of surface charges of gold nanoclusters on long-term in vivo biodistribution, toxicity, and cancer radiation therapy. *International Journal of Nanomedicine*, 11, 3475–3485.

Wang, Y., Liu, Y., Luehmann, H., Xia, X., Brown, P., Jarreau, C., … Xia, Y. (2012). Evaluating the pharmacokinetics and in vivo cancer targeting capability of Au nanocages by positron emission tomography imaging. *ACS Nano*, 6, 5880–5888.

Wang, Y., Liu, Y., Luehmann, H., Xia, X., Wan, D., Cutler, C., & Xia, Y. (2013a). Radioluminescent gold nanocages with controlled radioactivity for real-time in vivo imaging. *Nano Letters*, 13, 581–585.

Weis, S. M., & Cheresh, D. A. (2011). Tumor angiogenesis: Molecular pathways and therapeutic targets. *Nature Medicine*, 17, 1359–1370.

White, A. D., Nowinski, A. K., Huang, W., Keefe, A. J., Sun, F., & Jiang, S. (2012). Decoding nonspecific interactions from nature. *Chemical Science*, 3, 3488–3494. https://doi.org/10.1039/C2SC21135A

Wilczewska, A. Z., Niemirowicz, K., Markiewicz, K. H., & Car, H. (2012). Nanoparticles as drug delivery systems. *Pharmacological Reports*, 64, 1020–1037. https://doi.org/10.1016/S1734-1140(12)70901-5

Wiley, B., Sun, Y., Chen, J., Cang, H., Li, Z. Y., Li, X., & Xia, Y. (2005). Shape-controlled synthesis of silver and gold nanostructures. *MRS Bulletin*, 30, 356–361.

Wilhelm, S., Tavares, A. J., Dai, Q., Ohta, S., Audet, J., Dvorak, H. F., & Chan, W. C. (2016). Analysis of nanoparticle delivery to tumours. *Nature Reviews Materials*, 1, 16014. https://doi.org/10.1038/natrevmats.2016.14

Wong, A. C., & Wright, D. W. (2016). Size-dependent cellular uptake of DNA functionalized gold nanoparticles. *Small*, 12, 5592–5600.

Wong, C., Stylianopoulos, T., Cui, J., Martin, J., Chauhan, V. P., Jiang, W., … Fukumura, D. (2011). Multistage nanoparticle delivery system for deep penetration into tumor tissue. *Proceedings of the National Academy of Sciences of the United States of America*, 108, 2426–2431. https://doi.org/10.1073/pnas.1018382108

Xia, X., Monteiroriviere, N. A., & Riviere, J. E. (2010). An index for characterization of nanomaterials in biological systems. *Nature Nanotechnology*, 5, 671–675.

Xia, X., Yang, M., Wang, Y., Zheng, Y., Li, Q., Chen, J., & Xia, Y. (2012). Quantifying the coverage density of poly(ethylene glycol) chains on the surface of gold nanostructures. *ACS Nano*, 6, 512–522. https://doi.org/10.1021/nn2038516

Xiao, W., Xiong, J., Zhang, S., Xiong, Y., Zhang, H., & Gao, H. (2018). Influence of ligands property and particle size of gold nanoparticles on the protein adsorption and corresponding targeting ability. *International Journal of Pharmaceutics*, 538, 105–111. https://doi.org/10.1016/j.ijpharm.2018.01.011

Yameen, B., Choi, W. I., Vilos, C., Swami, A., Shi, J., & Farokhzad, O. C. (2014). Insight into nanoparticle cellular uptake and intracellular targeting. *Journal of Controlled Release*, 190, 485–499.

Yang, C., Uertz, J., Yohan, D., & Chithrani, B. D. (2014). Peptide modified gold nanoparticles for improved cellular uptake, nuclear transport, and intracellular retention. *Nanoscale*, 6, 12026–12033. https://doi.org/10.1039/C4NR02535K

Yang, M., Huo, D., Gilroy, K. D., Sun, X., Sultan, D., Luehmann, H., … Xia, Y. (2017). Facile synthesis of 64Cu-doped Au nanocages for positron emission tomography imaging. *ChemNanoMat*, 3, 44–50. https://doi.org/10.1002/cnma.201600281

Yang, Q., Jones, S. W., Parker, C. L., Zamboni, W. C., Bear, J. E., & Lai, S. K. (2014b). Evading immune cell uptake and clearance requires PEG grafting at densities substantially exceeding the minimum for brush conformation. *Molecular Pharmaceutics*, 11, 1250–1258. https://doi.org/10.1021/mp400703d

Yang, S., Sun, S., Zhou, C., Hao, G., Liu, J., Ramezani, S., … Zheng, J. (2015). Renal clearance and degradation of glutathione-coated copper nanoparticles. *Bioconjugate Chemistry*, 26, 511–519. https://doi.org/10.1021/acs.bioconjchem.5b00003

Yang, W., Ella-Menye, J. R., Liu, S., Bai, T., Wang, D., Yu, Q., … Jiang, S. (2014a). Cross-linked carboxybetaine SAMs enable nanoparticles with remarkable stability in complex media. *Langmuir*, *30*, 2522–2529. https://doi.org/10.1021/la404941m

Yang, X., Stein, E. W., Ashkenazi, S., & Wang, L. V. (2009). Nanoparticles for photoacoustic imaging. *WIREs Nanomedicine and Nanobiotechnology*, *1*, 360–368.

Yang, X., Yang, M., Pang, B., Vara, M., & Xia, Y. (2015). Gold nanomaterials at work in biomedicine. *Chemical Reviews*, *115*, 10410–10488.

Ye, D., Shuhendler, A. J., Cui, L., Tong, L., Tee, S. S., Tikhomirov, G., … Rao, J. (2014). Bioorthogonal cyclization-mediated in situ self-assembly of small molecule probes for imaging caspase activity in vivo. *Nature Chemistry*, *6*, 519–526.

Ye, S., Marston, G., McLaughlan, J. R., Sigle, D. O., Ingram, N., Freear, S., … Coletta, P. L. (2015). Engineering gold nanotubes with controlled length and near-infrared absorption for Theranostic applications. *Advanced Functional Materials*, *25*, 2117–2127.

Ye, X., Zheng, C., Chen, J., Gao, Y., & Murray, C. B. (2013). Using binary surfactant mixtures to simultaneously improve the dimensional tunability and monodispersity in the seeded growth of gold nanorods. *Nano Letters*, *13*, 765–771.

Yin, H., Mai, D., Gan, F., & Chen, X. (2014). One-step synthesis of linear and cyclic RGD conjugated gold nanoparticles for tumour targeting and imaging. *RSC Advances*, *4*, 9078–9085.

Yin, L., Yang, Y., Wang, S., Wang, W., Zhang, S., & Tao, N. (2015). Measuring binding kinetics of antibody-conjugated gold nanoparticles with intact cells. *Small*, *11*, 3782–3788. https://doi.org/10.1002/smll.201500112

Yoo, J., Chambers, E., & Mitragotri, S. (2010). Factors that control the circulation time of nanoparticles in blood: Challenges. *Solutions and Future Prospects. Current Pharmaceutical Design*, *16*, 2298–2307.

You, J., Zhou, J., Zhou, M., Liu, Y., Robertson, J. D., Liang, D., … Li, C. (2014). Pharmacokinetics, clearance, and biosafety of polyethylene glycol-coated hollow gold nanospheres. *Particle and Fibre Toxicology*, *11*, 26. https://doi.org/10.1186/1743-8977-11-26

Yu, M., & Zheng, J. (2015). Clearance pathways and tumor targeting of imaging nanoparticles. *ACS Nano*, *9*, 6655–6674. https://doi.org/10.1021/acsnano.5b01320

Yu, M., Zhou, C., Liu, J., Hankins, J. D., & Zheng, J. (2011). Luminescent gold nanoparticles with pH-dependent membrane adsorption. *Journal of the American Chemical Society*, *133*, 11014–11017. https://doi.org/10.1021/ja201930p

Zhang, C., Li, C., Liu, Y., Zhang, J., Bao, C., Liang, S., … Cui, D. (2015). Gold nanoclusters-based Nanoprobes for simultaneous fluorescence imaging and targeted photodynamic therapy with superior penetration and retention behavior in tumors. *Advanced Functional Materials*, *25*, 1314–1325. https://doi.org/10.1002/adfm.201403095

Zhang, G., Yang, Z., Lu, W., Zhang, R., Huang, Q., Tian, M., … Li, C. (2009). Influence of anchoring ligands and particle size on the colloidal stability and in vivo biodistribution of polyethylene glycol-coated gold nanoparticles in tumor-xenografted mice. *Biomaterials*, *30*, 1928–1936.

Zhang, K., Fang, H., Chen, Z., Taylor, J., & Wooley, K. L. (2008). Shape effects of nanoparticles conjugated with cell-penetrating peptides (HIV tat PTD) on CHO cell uptake. *Bioconjugate Chemistry*, *19*, 1880–1887.

Zhang, S., Li, J., Lykotrafitis, G., Bao, G., & Suresh, S. (2009). Size-dependent endocytosis of nanoparticles. *Advanced Materials*, *21*, 419–424. https://doi.org/10.1002/adma.200801393

Zhang, Y., Poon, W., Tavares, A. J., Mcgilvray, I. D., & Chan, W. C. W. (2016). Nanoparticle–liver interactions: Cellular uptake and hepatobiliary elimination. *Journal of Controlled Release*, *240*, 332–348.

Zhang, Y. R., Lin, R., Li, H. J., He, W. L., Du, J. Z., & Wang, J. (2018). Strategies to improve tumor penetration of nanomedicines through nanoparticle design. *WIREs Nanomedicine and Nanobiotechnology*, e1519. https://doi.org/10.1002/wnan.1519

Zhao, Y., Sultan, D., Detering, L., Luehmann, H., & Liu, Y. (2014). Facile synthesis, pharmacokinetic and systemic clearance evaluation, and positron emission tomography cancer imaging of 64Cu-Au alloy nanoclusters. *Nanoscale*, *6*, 13501–13509. https://doi.org/10.1039/C4NR04569F

Zhao, Y., Detering, L., Sultan, D., Cooper, M. L., You, M., Cho, S., … Dehdashti, F. (2016). Gold nanoclusters doped with 64Cu for CXCR4 positron emission tomography imaging of breast Cancer and metastasis. *ACS Nano*, *10*, 5959–5970.

Zheng, M., Davidson, F., & Huang, X. (2003). Ethylene glycol monolayer protected nanoparticles for eliminating nonspecific binding with biological molecules. *Journal of the American Chemical Society*, *125*, 7790–7791.

Zheng, M., Li, Z., & Huang, X. (2004). Ethylene glycol monolayer protected nanoparticles: Synthesis, characterization, and interactions with biological molecules. *Langmuir*, *20*, 4226–4235. https://doi.org/10.1021/la035981i

Zheng, Y., Zhong, X., Li, Z., & Xia, Y. (2014). Successive, seed-mediated growth for the synthesis of single-crystal gold Nanospheres with uniform diameters controlled in the range of 5-150 nm. *Particle & Particle Systems Characterization*, *31*, 266–273.

Zheng, Y., Ma, Y., Zeng, J., Zhong, X., Jin, M., Li, Z. Y., & Xia, Y. (2013). Seed-mediated synthesis of single-crystal gold Nanospheres with controlled diameters in the range 5–30 nm and their self-assembly upon dilution. *Chemistry, an Asian Journal*, *8*, 792–799.

Zhou, C., Long, M., Qin, Y., Sun, X., & Zheng, J. (2011). Luminescent gold nanoparticles with efficient renal clearance. *Angewandte Chemie International Edition*, *50*, 3168–3172. https://doi.org/10.1002/anie.201007321